Using $\delta^{13}C$-CH_4 and δD-CH_4 to constrain Arctic methane emissions

Nicola J. Warwick[1,2], Michelle L. Cain[1], Rebecca Fisher[3], James L. France[4], David Lowry[3], Sylvia E. Michel[5], Euan G. Nisbet[3], Bruce H. Vaughn[5], James W. C. White[5] and John A. Pyle[1,2]

[1]National Centre for Atmospheric Science, NCAS, UK.
[2]Department of Chemistry, University of Cambridge, Lensfield Road, Cambridge, CB2 1EW, UK.
[3]Department of Earth Sciences, Royal Holloway, University of London, Egham, TW20 0EX, UK.
[4]School of Environmental Sciences, University of East Anglia, Norwich, NR4 7TJ, UK.
[5]Institute of Arctic and Alpine Research (INSTAAR), University of Colorado, Boulder, CO 80309, USA.

Correspondence to: Nicola J. Warwick (Nicola.Warwick@atm.ch.cam.ac.uk)

Abstract. We present a global methane modelling study assessing the sensitivity of Arctic atmospheric CH_4 mole fractions, $\delta^{13}C$-CH_4 and δD-CH_4 to uncertainties in Arctic methane sources. Model simulations include methane tracers tagged~~coloured~~ by source and isotopic composition and are compared with atmospheric data at four high northern latitude measurement sites. We find the model's ability to capture the magnitude and phase of observed seasonal cycles of CH_4 mixing ratios, $\delta^{13}C$-CH_4 and δD-CH_4 in high northern latitudes is much improved using a later spring kick-off and autumn decline in high northern latitude wetland emissions than predicted by most process models. Results from our model simulations indicate that recent predictions of large methane emissions from thawing submarine permafrost in the East Siberian Arctic Shelf region could only be reconciled with global scale atmospheric observations by making large adjustments to high latitude anthropogenic or wetland emission inventories.

1 Introduction

Methane is an important greenhouse gas that has more than doubled in atmospheric concentration since pre-industrial times. Following a slow-down in the rate of growth in the late 1990s, the methane content of the atmosphere began increasing again in 2007 (Dlugokencky et al., 1998, Bousquet et al., 2011, Nisbet et al., 2014). Although this increase has occurred globally, latitudinal differences in methane growth rates suggest multiple causes for the renewed growth. In 2007, the Arctic experienced a rapid methane increase, but in 2008 and 2009-10 growth was strongest in the tropics. This renewed global increase in atmospheric methane has been accompanied by a shift towards more ^{13}C-depleted values, suggesting that one explanation for the change could be an increase in ^{13}C-depleted wetland emissions (Nisbet et al., ~~submitted~~2016). However, other factors such as changing emissions from ruminant animals (Schaefer et al., 2016) and the fossil fuel industry could also play a role (Bergamaschi et al., 2013, Kirschke et al., 2013, Hausmann et al., 2016).

The Arctic contains important methane sources that are currently poorly quantified and climate sensitive, with the potential for positive climate feedbacks. The largest and most uncertain of these are emissions from wetlands (e.g. Melton et al., 2013, Saunois et al., 2016). While wetland methane fluxes can be obtained experimentally by chamber studies and eddy correlation techniques (e.g. Pelletier et al., 2007, O’Shea et al, 2014), the heterogeneous conditions in wetlands and seasonal and interannual variation in wetland area (Petrescu et al., 2010) can lead to large uncertainties, both spatially and temporally, when upscaling this data. As high latitude wetland emissions are generally considered to occur from May melt to October freeze-up (Bohn et al., 2015, Christensen et al., 2003), and due to difficulties conducting field campaigns during the winter and spring-melt seasons, to~~-~~date most experimental Arctic wetland flux data has been reported for the summer season. However, a recent Arctic wetland study using year-round eddy flux data reported the presence of large methane emissions continuing well into winter, when subsurface soil temperatures remain close to 0°C (Zona et al., 2016). This study concluded that cold season (September-May) fluxes dominated the Arctic tundra methane budget.

Methane emissions from wetlands can also be estimated using process-based models. However, a recent model intercomparison study, WETCHIMP, showed wide disagreement in the magnitude of global and regional emissions among large-scale models (Melton et al., 2013). The magnitude of methane emissions from high northern latitude wetlands (>50° N) varied from 21 to 54 Tg yr^{-1} (Melton et al., 2013), representing approximately 5 to 10 % of the total global methane emission budget. There was also significant variability between models in the seasonal distribution of these emissions. Figure 1 shows a comparison of seasonal cycles of high northern latitude wetland emissions from the WETCHIMP models, the wetland dataset described in Fung et al. (1991) and the model inversion study of Bousquet et al. (2011). There is significant spread in how the emissions are distributed throughout the year, with the summertime peak in emissions occurring in June, July or August depending on the model considered. In a model intercomparison focusing on wetland emissions in West Siberia (WETCHIMP-WSL, Bohn et al., 2015), the largest disagreement in the temporal distribution of emissions occurs in springtime (May and June). During this period, the range in normalised model monthly emissions spans from a minimum of negative values (representing methane uptake) to a peak in the emission seasonal cycle. This large uncertainty associated with the timing of, and processes controlling, seasonal variations in wetland methane emissions needs to be resolved before predictions can be made of how emissions might change in a changing climate.

Decomposing gas hydrates may also represent a small, but significant, climate sensitive methane source. Shallow methane hydrates in Arctic regions may be particularly vulnerable to destabilisation following increases in temperature as a result of climate change. Furthermore, thawing permafrost could release methane previously trapped below in shallow reservoirs, including hydrates, to the atmosphere. Previous studies of the methane budget have either omitted a hydrate source or used a global value for Arctic hydrate emissions of 5 Tg yr^{-1}. However this value is no more than a placeholder suggested by Cicerone and Oremland (1988). More recently, Shakhova et al., (2010) and Shakhova et al. (2014) used ship-based observations to estimate methane emissions from thawing permafrost on the East Siberian Arctic Shelf (ESAS). They estimated a total ESAS methane source from diffusion, ebullition and storm-induced release from subsea permafrost and hydrates of 17 Tg yr^{-1}; significantly more than the 5 Tg yr^{-1} suggested by Cicerone and Oremland (1988). However, a recent study by Berchet at al. (2016) using an atmospheric chemistry transport model, found that an ESAS source as high as 17 Tg yr^{-1} was inconsistent with atmospheric observations of methane mole fractions at northern high latitude measurement sites. In the~~is~~ Berchet et al. (2016) study, ESAS emissions were estimated to be in the range 0.5 to 4.3 Tg yr^{-1}.

Other recent studies identifying additional potential northern high latitude sources and sinks of methane include emissions from Arctic thermokarst lakes (11.86 Tg yr^{-1}, Tan and Zhuang, 2015), polymers in oceanic ice (~7 Tg yr^{-1}, Kort et al., 2012) and methane uptake by boreal vegetation (~-9 Tg yr^{-1}, Sundqvist et al., 2012). These studies have either used process-based models or extrapolated local observations to calculate Arctic fluxes that would all be highly significant on a regional scale. However, uncertainties in these sources are high as many fluxes may be episodic as well as spatially scattered, and could therefore be missed by relatively infrequent field campaigns. In addition to natural sources, the Arctic contains methane emissions from some of the world's largest gas producing plants, situated in northern Russia (Reshetnikov et al., 2000; EDGAR v4.2, http://edgar.jrc.ec.europa.eu, 2011).

The main atmospheric sink of methane is reaction with the hydroxyl radical, OH. Other lesser sinks include reaction with Cl in the boundary layer (e.g. Allan et al., 2007, Lawler et al., 2011, Banton et al., 2015), reaction with Cl and O(^{1}D) in the stratosphere and uptake of methane by methanotrophs in oxic soils. These sinks all vary seasonally due to seasonal changes in solar insolation and temperature etc..~~, with peak destruction rates during the summer~~. Overall, knowledge of source and sink partitioning within the Arctic methane budget is poor, and a better understanding of emissions is required to determine the best emission reduction strategies and feedbacks in a future climate.

Along with atmospheric modelling, measurements of methane mole fractions provide important information on the geographic and seasonal distribution of methane emissions. However, mole fraction measurements alone do not give us the ability to distinguish between emissions from different methane sources. This can be achieved in a broad sense using observations of stable isotope ratios in methane as different sources have distinct isotopic ratios. For example, methane emitted from wetlands is relatively more depleted in ^{13}C than that from fossil sources, which are in turn depleted relative to methane derived from biomass burning (Dlugokencky et al. 2011). To date, global atmospheric modelling studies have only incorporated information on the $^{13}C/^{12}C$ ($\delta^{13}C_{CH4}$) composition of methane using geographically uniform source isotopic signatures. However, new information on the atmospheric distribution of the D/H composition (White et al., 2016) provides an additional potential discriminant between source~~s~~ and sink~~ource~~ strengths. Rigby et al. (2012) included both $^{13}CH_4$ and CH_3D tracers in an atmospheric model to quantify uncertainty reductions in future methane emission estimates that could be achieved if measurement networks performed high-frequency and precision isotopic measurements. However, model results were not compared to existing atmospheric isotopic data in this study. Here we present the first modelling study of modern methane to (a) include published large geographical variations in the isotopic signature of wetland emissions and (b) assess methane emission scenarios against atmospheric observations of δD_{CH4}.

Global model simulations are performed using the p-TOMCAT 3D chemistry transport model using offline chemistry (Warwick et al., 2006) and multiple methane tracers tagged~~coloured~~ by source and δ^{13}C and δD isotopic composition. We investigate the sensitivity of atmospheric distributions of CH_4, $\delta^{13}C_{CH4}$ and δD_{CH4} to changes in fluxes from climate-sensitive Arctic sources and analyse potential causes of differences between models and measurements in this region.

2 Measurements

Model results are compared to monthly mean weekly flask observations of CH_4 mixing ratios, $\delta^{13}C$-CH_4 and δD-CH_4 from NOAA-ESRL sampling sites at Alert (82°N, 63°W), Ny-Alesund (79°N, 12°E), Barrow (71°N, 157°W) and Cold Bay (55°N, 163°W) (Dlugokencky et al., 2013; White and Vaughn, 2015; White et al., 2016). These sites were selected for comparison as they are the four most northerly sites with simultaneous CH_4, $\delta^{13}C$-CH_4 and δD-CH_4 observation data. In addition, modelled latitudinal gradients of CH_4, $\delta^{13}C$-CH_4 and δD-CH_4 are analysed by comparison with annual mean observations from a further 8 NOAA-ESRL sampling sites spread over latitudes 90° S to 53° N. The location of these measurement sites is shown in Figure 3 (due to the proximity of the measurement sites at Mauna Loa and Cape Kumukahi they appear as one point). Monthly mean observations are averaged over the years 2005 to 2009 (the period for which there is δD-CH_4 data available). NOAA-ESRL was responsible for the collection of the sample and logistics, with cooperating agencies. Samples were then analysed for methane mixing ratios at NOAA-ESRL in Boulder, Colorado, with an analytical repeatability of 0.8 to 2.3 ppb. Stable isotopic compositions were determined at the Stable Isotope Laboratory at INSTAAR, part of the University of Colorado, Boulder, with a precision of better than 0.1 ‰ for $\delta^{13}C$-CH_4 (White et al., 2015; Miller et al., 2002) and 2‰ for δD-CH_4 (White et al., 2016).

3 Isotopic composition of methane

The isotopic composition of atmospheric methane is generally expressed in ‘delta’ notation, as the isotopic ratio in the sample compared to an international standard. The original standard for the $^{13}C/^{12}C$ ratio was Pee Dee Belemnite, a fossil from the Pee Dee marine carbonate formation in South Carolina (Craig, 1957), which established the V-PDB scale. For the D/H ratio, the international standard is Vienna Standard Mean Ocean Water (VSMOW) (DeWitt et al., 1980). The delta values for the two main stable isotopologues of methane are given by

$$\delta^{13}C = 1000\left(\frac{R_{13CH4}}{R_{PDB}} - 1\right) \qquad (1)$$

$$\delta D = 1000\left(\frac{R_{CH3D}}{R_{VSMOW}} - 1\right) \qquad (2)$$

where R_x is the molar ratio of ^{13}C or D to the most abundant isotopologue (i.e. ^{12}C or H respectively). R_{PDB} is the $^{13}C/^{12}C$ ratio found in V-PDB and R_{VSMOW} is the D/H ratio found in V-SMOW. Global mean surface atmospheric observations of CH_4, $\delta^{13}C$-CH_4 and δD-CH_4 were ~1780 ppb,~-47.2 ‰ and ~-86 ‰ respectively for the 2005 to 2009 period (Dlugokencky et al., 2013; White and Vaughn, 2015; White et al., 2016). Geographical and altitudinal variations in these compositions arise as a result of variations in the distributions of the isotopic composition of the parent organic matter, the method of production (pyrogenic, thermogenic or biogenic) and differing rates of destruction between methane isotopologues. At large scales, the δD composition of methane is controlled by the δD of water present, while at smaller scales, the methods of production and destruction may play a more important role. Likewise the $\delta^{13}C$ composition of methane can be influenced by the type of parent organic matter (e.g. C3 or C4 vegetation), as well as the method of production. As different methane sources tend to have distinct isotopic ratios, observations of the isotopic composition of atmospheric methane can be used as additional constraints on the methane budget (e.g. Rigby et al., 2013; Schaefer et al, 2016).

4 Model description

The global 3D chemical transport model, p-TOMCAT, has been used extensively for tropospheric studies and is described in more detail in Cook et al. (2007) and Warwick et al. (2013). For this study, the model was run at a horizontal resolution of ~2.8° x 2.8°, with 31 levels extending from the surface to 10 hPa. The horizontal and vertical transport of tracers was based on 6-hourly meteorological fields, including winds and temperatures derived from the operational analyses of the European Centre for Medium Range Weather Forecasts (ECMWF) for 2009.

The version of p-TOMCAT used in this work has been modified to include parameterised chemistry where tagged~~coloured-~~source-type methane tracers of $^{12}CH_4$ and $^{13}CH_4$, and a 'total' CH_3D are destroyed via reaction with OH, O(^{1}D) and Cl. The OH distributions are prescribed hourly values taken from a full chemistry version of p-TOMCAT and compare well with other global OH distributions described in the literature, giving a global methane lifetime of 10.4 years with respect to OH (for more details see Warwick et al., 2006). A comparison of modelled seasonal cycles of methyl chloroform and observational data from the NOAA-ESRL halocarbons in situ program at Barrow, Alaska, suggests that the seasonal cycle of the model prescribed OH concentrations is well represented in the Arctic region (see Fig. S1~~2~~). Although there is a slight difference in the timing of the observed and modelled methyl chloroform minima, the modelled seasonal cycle falls well within the range of observations. The stratospheric destruction of methane by reaction with Cl and O(^{1}D) is derived from prescribed 2D Cl and O(^{1}D) 5 day mean distributions taken from the Cambridge 2D model (Bekki and Pyle, 1994). Mixing ratios of Cl in the marine boundary layer are prescribed with latitudinal and seasonal variations according to Allan et al., (2007). Global atmospheric methane lifetimes with respect to the Cl and O(1D) stratospheric and Cl marine boundary layer reactions are 265 and 360 years respectively. Reaction rate coefficients for the reaction of CH_4 with OH is taken from Burkholder et al. (2015) , and with O(1D) and Cl from Atkinson et al. (2004). Kinetic isotope effects (KIEs, defined as the ratio of rate constants for the reactions involving the reactant and an isotopically substituted reactant with a certain species) for the methane reaction rates are included in the model chemistry scheme and are listed in Table S1. Oxidation of methane by soils is treated as a negative emission following Fung et al., (1991).

Methane emissions and source-specific isotopic signatures used in the p-TOMCAT BASE control scenario are described in Table 1~~S2~~. The geographical and seasonal distribution of methane fluxes are taken from EDGAR v4.1 (http://edgar.jrc.ec.europa.eu/overview.php?v=41) for 2005, Fung et al. (1991) and Van der Werf et al. (2006). The geographical distribution of wetland emissions above 50° N is shown in Fig. 2. Further details on the fluxes and source-specific isotopic signatures used in the model are outlined in the Supplementary Online Material. Methane tracers of $^{12}CH_4$, $^{13}CH_4$ and CH_3D are tagged by source type as shown in Table 1. In addition, the 'Northern Wetlands' tracer is also tagged by continental region, with emission regions split into North American, North European or north Asian. Different emission and sink scenarios considered in this study and their variations from the BASE scenario are described in later sections and listed in Table 2.

Initially, a ‘total’ methane tracer was spun-up in a 40-year single-tracer simulation until calculated year-to-year changes in local methane mole fractions were negligible. The tagged~~coloured~~ methane source tracers in each scenario were then initialised by scaling this spun-up total methane tracer globally, according to the global emission fraction and isotopic composition of the source. Results presented here are taken from the final year of further 40-year simulations using perpetual 2009 meteorology, after which year-to-year changes in the local mole fractions of the individual tracers were deemed to be negligible (<0.5 %), along with the associated changes in δ^{13}C-CH$_4$ and δD-CH$_4$.

5 Atmospheric distribution of methane mole fraction and isotopic composition

5.1 Global distribution

Figure 3 shows the modelled annual mean surface distributions of total CH$_4$, δ^{13}C-CH$_4$ and δD-CH$_4$ for the BASE scenario. The results are broadly comparable to observational data, with higher mixing ratios and lighter (more negative) isotopic fractionations occurring in the Northern Hemisphere (NH) than the Southern Hemisphere (SH). This gradient in isotopic fractionations arises as the rates of reaction of OH, Cl and O(^{1}D) with ^{13}CH$_4$ and CH$_3$D are all fractionally slower than with ^{12}CH$_4$ (see Table S1). Therefore, both δ^{13}C and δD increase (become more enriched in the heavy isotope) with increased exposure to atmospheric sinks. As the majority of methane emissions are located in the NH, and because these are predominantly depleted in heavy isotopes, there are strong latitudinal gradients in methane and its isotopic fractionations: higher concentrations and more negative δ^{13}C-CH$_4$ and δD-CH$_4$ values are found in the NH than the SH. Regional variations in δ^{13}C-CH$_4$ and δD-CH$_4$ also occur due to regional variations in methane source types with differing isotopic signatures (see Table 1~~S2~~).

The model captures the observed latitudinal gradients in CH$_4$, and δ^{13}C-CH$_4$ (see Fig. 4). The latitudinal gradient in δD-CH$_4$ is also well represented, except for a step change between the South Pole and lower southern latitudes in the observations that is not captured by the model. One reason for this could be errors in the model scenario. However, given the well-mixed nature of both SH CH$_4$ mixing ratios and δ^{13}C-CH$_4$values, the limited amount of δD-CH$_4$ data available, and the precision of the measurements, it is also possible that this step change in the SH latitudinal gradient maybe due to noise in the measurement data. ~~and δD-CH$_4$, although the gradient in δD-CH$_4$ is underestimated in the model in northern mid-latitudes (see Fig. 5).~~

The~~se~~ latitudinal gradients of CH$_4$, δ^{13}C-CH$_4$ and δD-CH$_4$ are likely to be strongly influenced by the representation of Arctic methane sources, particularly high latitude wetland emissions, which will give a strong isotopic atmospheric signal due to their very negative δ^{13}C-CH$_4$ and δD-CH$_4$ values. The sensitivity of the modelled latitudinal gradient to variations in particular Arctic methane sources is discussed in more detail in Sect. 6.

5.2 Arctic seasonal cycles

5.2.1 Comparison of the base simulation with observations

The observed seasonal cycle of CH_4 mole fractions in high northern latitudes is dominated by a sharp summer minimum in July, and a broader winter maximum from October to March (see Fig. 5). This seasonal cycle arises as a result of seasonal variations in the major methane sink, reaction with OH, seasonal variations in the surface sources of methane and seasonal changes in vertical mixing and horizontal transport. For example, the Arctic is influenced by long-range transport of airmasses containing high levels of anthropogenic methane from lower latitudes during winter and spring (e.g. Dlugokencky et al. 1995; Worthy et al. 2009). Model studies have had difficulty capturing seasonal cycles of methane in high northern latitudes (e.g. Houweling et al., 2000; Wang et al., 2004; Pickett-Heaps et al., 2011), in particular the timing of the summer minimum.

Observed seasonal cycles of $\delta^{13}C$-CH_4 and δD-CH_4 show some level of anti-correlation with CH_4 mole fractions. If the observed seasonal cycle of CH_4 were due to reaction with OH alone, then the KIEs of the CH_4 + OH reaction would result in $\delta^{13}C$-CH_4 and δD-CH_4 seasonal cycles 180° out of phase with the CH_4 seasonal cycle: the minimum in CH_4 mixing ratio corresponding to maxima in $\delta^{13}C$-CH_4 and δD-CH_4. However, phase relationships between observed seasonal cycles in CH_4, $\delta^{13}C$-CH_4 and δD-CH_4 are also influenced by seasonal variations in surface sources and lesser, alternate sinks leading to more complicated phase relationships.

The reaction of CH_3D with OH has a larger KIE than the reaction of $^{13}CH_4$ with OH (see Table S1). Therefore seasonal variations in atmospheric δD-CH_4 will tend to be more dominated by seasonal changes in the OH sink than $\delta^{13}C$-CH_4, with atmospheric $\delta^{13}C$-CH_4 being relatively more influenced by sources. Figure 5 shows that the observed seasonal cycle of δD-CH_4 is approximately anti-correlated with CH_4, as would be expected for a seasonal cycle controlled by seasonal variations in OH. However, this is not true for $\delta^{13}C$-CH_4. There is an offset between the CH_4 and $\delta^{13}C$-CH_4 seasonal cycles, with a period in late spring where CH_4 decreases and there is either no change or a slight decrease in $\delta^{13}C$-CH_4. In addition, a simultaneous increase in both observed CH_4 and $\delta^{13}C$-CH_4 from October through to the end of the year demonstrates that factors other than seasonal variations in OH play a role in determining the seasonal cycle of $\delta^{13}C$-CH_4.

Figure 5 also shows a comparison of modelled seasonal cycles of CH_4, $\delta^{13}C$-CH_4 and δD-CH_4 from the BASE scenario with observational data from four high northern latitude sites. Although the model captures the phase and magnitude of observed seasonal cycles in lower northern latitudes (e.g. Cold Bay), clear differences in the magnitude and/or phase are evident in higher latitudes (Alert, Ny-Alesund, Barrow). Analysis of the regionally tagged tracers for wetland emissions >50°N (North American, North European and North Asian), indicate that modelled seasonal cycles at all four measurement sites are predominantly influenced by American, and to a lesser extent European wetland emissions, with little sensitivity to Asian wetland emissions. The model is unable to capture the magnitude and timing of the Arctic summer minimum in CH_4 mixing ratios, while the modelled summer decrease in $\delta^{13}C$-CH_4 and δD-CH_4 occurs earlier than observed. In addition, the model underestimates the amplitude of the observed Arctic seasonal cycle in δD-CH_4. These discrepancies point to errors in the representation of Arctic methane sources and/or the isotopic signature data used within the model, particularly in American and/or European regions. In Sect. 6, we investigate the sensitivity of modelled seasonal cycles to uncertainties in the δD KIE for the CH_4 + OH reaction, as well as adjustments in the phase and magnitude of certain Arctic sources.

6 Model sensitivities to Arctic source magnitudes and δD isotopic signatures and fractionations

6.1 Model sensitivity to $KIE^{H/D}$ and the wetland δD signature

Although the model is able to capture the phase and magnitude of observed seasonal cycles of methyl chloroform in the Arctic, suggesting that the OH seasonal cycle is well represented (Fig. S1), the model underestimates the amplitude of Arctic seasonal cycles of both CH_4 and δD-CH_4 (Fig. 5). In two further separate model simulations, we investigated the sensitivity of Arctic modelled seasonal cycles in δD-CH_4 to (a) uncertainities in the KIE of the CH_3D + OH reaction and (b) uncertainties in the δD signature of methane emissions from high northern latitude wetlands.

Literature KIE values for $k^{CH4+OH}/k^{CH3D+OH}$ range from 1.16 to 1.3, clustering at the higher end of range (DeMore et al., 1993; Gierczak et al., 1997; Bergamaschi et al., 2000; Saueressig et al., 2001; Tyler et al., 2007). In a separate model simulation run parallel to the BASE simulation (DEC_KIE), we find that altering the $KIE^{CH3D+OH}$ reaction within the literature range has an important impact on modelled global mean δD-CH_4 values. However, we found the impact of varying $KIE^{CH3D+OH}$ on the magnitude of the modelled δD-CH_4 seasonal cycle to be negligible, offering no improvement over the BASE scenario when comparing with observations.

While there is now an increasing amount of data on $^{13}C/^{12}C$ source ratios, D/H ratios for methane sources have been less comprehensively studied and are therefore subject to larger uncertainties. Literature estimates of the δD-CH_4 isotopic signature from high northern latitude wetlands range from approximately -300 ‰ to -450 ‰ (e.g. Kulmann et al., 1998; Quay et al, 1999; Nakagawa et al., 2002; Umezawa et al., 2012). However, bulk regional δD values for western Siberian emissions estimated by Yamada et al. (2005) (-482 ‰ to -420 ‰, including the major wetland and fossil fuel sources) suggest a more negative δD signature for wetlands than determined by other studies. Here, in an additional simulation (WETLD_δD), we found that increasing the isotopic signature of >50° N wetland emissions from -360 ‰ to -500 ‰ improved the ability of the model to capture the magnitude of the observed seasonal cycle and latitudinal gradient of δD-CH_4 (not shown). However, using such a negative δD signature for high northern latitude wetland emissions would obviously shift the model global mean δD-CH_4 to more negative values, and would therefore have to be balanced by further altering the source/sink scenario. In addition, while altering the δD wetland source signature improves the representation of the modelled δD-CH_4 seasonal cycle, it does not impact the differences between the modelled and observed CH_4 seasonal cycles.

6.2 Model sensitivity to the wetland source

6.2.1 Varying the source magnitude

Emissions from high northern latitude wetlands (>50° N) are assigned a highly ^{13}C-depleted and D-depleted isotopic signature (~-70 ‰ and ~-360 ‰ respectively) in the model, as well as a strong seasonal cycle, peaking during the NH summer. Therefore reducing methane emissions from high latitude wetlands in early summer could potentially improve the comparison between observed and modelled seasonal cycles of CH_4, $\delta^{13}C$-CH_4 and δD-CH_4. Figure 6 shows the influence of varying the magnitude of the wetland source above 50° N on the phase and magnitude of modelled high latitude NH CH_4 and $\delta^{13}C$-CH_4 seasonal cycles. No results for δD-CH_4 are shown as CH_3D was not tagged~~coloured~~ by source in the model due to computer integration time limitations.

When the tagged~~coloured~~ high northern latitude (>50° N) wetland methane tracer (with emissions of 30 Tg yr^{-1}) is excluded from the model simulation (NO_WETLD scenario), the summer minimum in CH_4 mole fraction occurs later in the year (August/September) than in the BASE scenario and the seasonal variation in $\delta^{13}C$-CH_4 is substantially reduced (Fig. 6). When high northern latitude wetland emissions are increased by 50 % (i.e. the annual source strength is increased to 45 Tg yr^{-1}, INC_WETLD~~_X2~~ scenario), the summer minimum occurs earlier in the year (May/June) and seasonal variations in both CH_4 and $\delta^{13}C$-CH_4 increase relative to the BASE scenario (Fig. 6). Neither wetland scenario provides any improvement in the model's ability to capture observed seasonal cycles: the comparison with observations is worse when high northern latitude wetland emissions are removed, and there are only small changes to model results when high northern latitude wetland emissions are increased by 50 %. We found that altering the Fung et al. (1991) emission distribution in a simple way by varying the relative strengths of the three regional high northern latitude wetland tracers (North American, North European and North Asian) offered no improvement in the agreement between modelled and observed atmospheric seasonal cycles. Modelled seasonal cycles at the measurement station locations showed little sensitivity to emissions from north Asia (including Siberia, see Section 5.2.1), and increasing/decreasing the emission contribution from North America and Northern Europe gave similar results to the INC_WET and NO_WET scenarios.

Figure 7 shows the influence of varying the strength of wetland emissions above 50° N on the modelled latitudinal gradients of CH_4 and $\delta^{13}C$-CH_4. Removing this source completely dramatically reduces the ability of the model to capture observed latitudinal gradients: the modelled interpolar gradient in $\delta^{13}C$-CH_4 is reduced by ~75 % from ~0.4 ‰ to 0.1 ‰, and the gradient in CH_4 mixing ratios by ~22 % in the NO_WETLD scenario relative to the BASE scenario. Increasing high northern latitude wetland emissions by 50 % increases the interpolar difference in both CH_4 and $\delta^{13}C$-CH_4 in the INC_WETLD~~_X2~~ scenario relative to the BASE scenario. In this case, the gradient in CH_4 mole fractions is then slightly overestimated.

6.2.2 Varying the phase of the seasonal cycle

To investigate the impact of the prescribed phase of the seasonal cycle of high latitude wetland methane emissions on modelled atmospheric distributions of CH_4, $\delta^{13}C$-CH_4 and δD-CH_4, a further model scenario is run (DEL_WET) in which the seasonal cycle of this source is delayed by one month, resulting in a later spring kick-off in emissions and a decline in emissions that occurs later in autumn than in the BASE scenario. While this has a negligible influence on the modelled latitudinal gradient (not shown), ~~shifting~~delaying the high latitude wetland emission seasonal cycle~~ forward in the year~~ by one month (so the summer emission season starts and finishes one month later in the year) has a notable impact on modelled seasonal variations in atmospheric methane and its isotopic composition (see Fig. 8). In this case, the model is better able to capture observed seasonal cycles in CH_4, $\delta^{13}C$-CH_4 and δD-CH_4.

These results do not support the existence of a large spring burst in wetland emissions as has been reported in other studies (e.g. Christensen et al., 2004; Song et al., 2012). To capture the correct timing of the CH_4 minima and $\delta^{13}C$-CH_4 and δD-CH_4 maxima, the model requires that there be no large contribution from wetland emissions until June, with peak emissions occurring between July and September~~.~~ (see Figure 1, Fung_Del scenario) Equally, to capture the correct timing of the summer/autumn increase in CH_4 mixing ratios and decrease in $\delta^{13}C$-CH_4, the model requires strong contributions from an isotopically light source continuing through to October. This could be from autumnal wetland emissions, as represented here. A large late-autumnal high northern latitude wetland source is supported by the recent work of Zona et al., (2016), who observed strong methane fluxes at an Arctic wetland site continuing well after the near-surface soil layer starts to freeze in late August or early September. Alternatively, it is possible that the comparison between modelled and observed $\delta^{13}C$-CH_4 (though not CH_4 mixing ratios) could be improved by prescribing a seasonal variation to the signature of high northern latitude wetland emissions as observed by Sriskantharajah et al. (2012).

Figure 1 shows that the seasonal cycle of the Fung_Del emissions used in the DEL_WET scenario is similar in phase to that generated by the LPJ-Bern model (Melton et al., 2013), with an emission peak occurring later in the year than other datasets. In a comparision of the FUNG and LPJ-Bern wetland emission datasets we found that the difference in emission seasonal cycles at 50-90°N is a consistent feature over these latitudes, rather than a result of differing geographical emission distributions between the two datasets. In an intercomparison of wetland methane emission models over West Siberia (WETCHIMP-WSL, Bohn et al., 2015), the late August peak in Siberian emissions in LPJ-Bern was found to be due to a late peak in wet mineral soil intensity, supplemented by a late peak in CH_4-producing area. The August peak in LPJ_Bern West Siberian emissions in WETCHIMP-WSL was in agreement with the Bousquet et al. (2011) atmospheric model inversion study.

6.3 Model sensitivity to the hydrate / thawing permafrost source

Methane emissions from ocean bottom decomposing hydrates and thawing permafrost in the Arctic are not well known due to uncertainties in the amount of carbon in permafrost, the sizes and locations of the methane hydrate deposits, the rate of heat transfer through the ocean and sediments, and the fate of methane once it has been released into sea water (O'Connor et al. 2010). A recent study by Shakhova et al. (2014) estimated methane emissions of 17 Tg yr^{-1} from the ESAS based on extrapolation of field observations in the Southern Laptev Sea. An emission of this magnitude represents a substantial reassessment of the high northern latitude methane budget, being equivalent to ~25 % of total estimated methane emissions above 50° N. A subsequent study by Berchet et al. (2016) reported that an ESAS flux of this magnitude was inconsistent with atmospheric observations, and used a statistical analysis of observations and model simulations to estimate an ESAS source of 0.5 to 4.3 Tg yr^{-1}.

To assess the sensitivity of the model to uncertainties in this high latitude methane source, we compare three scenarios in which methane emissions from the East Siberian Arctic Shelf region are assigned magnitudes of 0, 5 and 17 Tg yr^{-1} (NO_HYD, BASE and INC_HYD scenarios respectively). These emissions are set to be constant throughout the year as about 10 % of the ESAS remains open water in winter due to the formation of polynyas, implying that it could be a source of CH_4 to the atmosphere year-round (Shakhova et al. 2015), and due to the lack of any further data on seasonality. However, it is possible that summer ESAS fluxes, when the region is ice-free, could be larger than winter fluxes (Berchet et al. 2016). The influence of these changes in emissions on the modelled latitudinal gradient is shown in Fig. 9. Although the magnitude of change in emission is small in comparison to the global budget (<~3 %), varying the strength of the ESAS source has a notable impact on modelled interpolar differences as the source is highly localised at high latitudes. In the scenario in which East Siberian Arctic Shelf emissions have been removed (NO_HYD), northern high latitude gradients in modelled CH_4 and $\delta^{13}C\text{-}CH_4$ are underestimated relative to observations. This demonstrates that the model does require a small, very high latitude, isotopically light source to capture observed latitudinal gradients, given the prescribed geographical distributions of emissions from other high latitude sources used in the BASE scenario. However, when ESAS hydrate emissions are increased to 17 Tg yr^{-1} (INC_HYD), the model predicts a larger latitudinal gradient in CH_4 between mid and high northern latitudes than seen in the observations (Fig 9). This remains true when using modelled mixing ratios from measurement site locations, rather than a zonal mean (not shown). Therefore our model simulations do not support the existence of an East Siberian Arctic Shelf methane source of this magnitude, given the representations of other methane sources outlined in Table 1 ~~S2~~.

It is, however, possible that an East Siberian Arctic Shelf source of 17 Tg yr^{-1} could be accommodated in our model set-up if adjustments were made to the representation of other high northern latitude sources within the model. At 30 Tg yr^{-1}, wetlands represent the largest single methane source in high latitude regions (Table 1~~S2~~), and therefore have the largest potential for flux adjustment. We consider an alternative scenario (WET_HYD) including emissions of 17 Tg yr^{-1} from the East Siberian Arctic Shelf, but only 18 Tg yr^{-1} from high northern latitude wetlands (i.e. high northern latitude wetland emissions are geographically uniformly reduced by 12 Tg yr^{-1} and total NH emissions remain the same as in the BASE scenario). In this case, the modelled zonal mean latitudinal gradient of CH_4 is in better agreement with the observations than INC_HYD (Fig. 9), and modelled mixing ratios from measurement site locations have very close agreement with observations. However in WET_HYD, the zonal mean latitudinal gradient in $\delta^{13}C\text{-}CH_4$ is reduced relative to both observations and the BASE scenario in northern mid-latitudes (Fig. 9). When WET_HYD modelled mixing ratios from measurement station locations are used rather than a zonal mean, this reduction in gradient is more apparent. This occurs as the isotopic signature of hydrate/permafrost emissions assigned in the model is larger than that of high latitude wetland emissions (~-55 ‰ compared to ~-70 ‰, see discussion below). In addition to the impact on the latitudinal gradient, the agreement of the model with observed seasonal cycles of CH_4, $\delta^{13}C-CH_4$ and $\delta D-CH_4$ is also reduced in high northern latitudes following the 12 Tg yr^{-1} reduction in high northern latitude wetland emissions (not shown). However, this is based on the use of constant ESAS emissions and inclusion of a seasonal cycle may influence our results. For example, if ESAS emissions with a $\delta^{13}C$ isotopic signature of -55 ‰ were assigned a seasonal cycle that peaked during the summer, along with wetland emissions, then this would likely lead to smaller differences in modelled seasonal cycles between WET_HYD and BASE.

These results are, at least partly, based on the assumption that the isotopic signatures assigned to high northern latitude wetlands and ocean floor hydrates/thawing permafrost are correct, and specifically that the $\delta^{13}C$ signature for wetland emissions is more negative than that for hydrates/permafrost. $\delta^{13}C$ signatures for Arctic wetland emissions have been determined in a number of studies and there is strong agreement that these emissions are highly depleted in ^{13}C, with values <-65 ‰ (Fisher et al., 2011, Sriskantharajah et al., 2012, O'Shea et al., 2014). Our value of -70 ‰ is based on recent data from the NERC MAMM (Methane in the Arctic: Measurements, process studies and Modelling) campaign (O'Shea et al., 2014). $\delta^{13}C$ signatures from ocean floor hydrates and permafrost are less well known and as far as we are aware, have not been published for the Laptev Sea region. Measurements taken from decomposing CH_4 hydrate in sediment cores in the Norwegian Arctic show a wide $\delta^{13}C$ isotopic range, from ~-72 ‰ to ~-46 ‰ (Milkov, 2005; Vaular et al., 2010, Fisher et al., 2011). However, methane released from the sea floor will be oxidised in the water column and enriched in ^{13}C before reaching the atmosphere as methanotrophs in ocean water would preferentially consume the lighter isotope. Therefore the isotopic signature of emission to the atmosphere will be more enriched in ^{13}C (less negative $\delta^{13}C$) than the $\delta^{13}C$ values from sediment cores (Graves et al., 2015). A substantially lighter isotopic signature for ESAS methane emissions, as would be required to capture atmospheric $\delta^{13}C-CH_4$ observations, is possible, however it would require both (a) a very light initial isotopic composition on release at the sea floor and (b) very limited oxidation in the water column before release to the atmosphere. These factors could be achieved with a shallow sea floor (as is present for the ESAS) and the formation of large methane bubbles.

To assess how a more negative $\delta^{13}C$ signature for ESAS hydrate/permafrost emissions would influence our model results, we construct a further scenario for $\delta^{13}C-CH_4$, WET_HYD_$\delta^{13}C$, in which the ESAS source of 17 $Tgyr^{-1}$ is assigned a $\delta^{13}C$ signature of -70 ‰. In this case, the model simulates a much larger latitudinal gradient in $\delta^{13}C-CH_4$ in high northern latitudes than is seen in the observations (Fig. 9). The agreement of the WET_HYD_$\delta^{13}C$ scenario with observed seasonal cycles of CH_4, $\delta^{13}C-CH_4$ and $\delta D-CH_4$ is reduced relative to BASE in high northern latitudes (not shown). However this is based on using constant aseasonal ESAS emissions in the model. If a seasonal cycle peaking during the summer was applied to ESAS emissions, it would likely become harder to distinguish between atmospheric CH_4 and $\delta^{13}C-CH_4$ seasonality due to ESAS emissions and that due to high latitude wetland emissions in our study as both emission datasets would have similar seasonal cycles and δ^{13}C isotopic compositions. Therefore, whether an ESAS source of 17 Tgyr^{-1} can be accommodated in our global model along with a reduction in high northern latitude wetland emissions is highly dependent on the δ^{13}C signature used for the respective sources, as well as potentially the seasonal cycle applied to the ESAS emissions. Our model simulations indicate that if the ESAS source has a very negative δ^{13}C signature (-70 ‰ or more negative), then such a large, localised, high latitude source would strongly influence global scale hemispheric gradients.

The sum of all other (mostly anthropogenic) sources >50° N is ~37 Tg yr^{-1} (see Table 1~~S2~~). The isotopic compositions of these sources are all either similar to, or heavier than the isotopic signature assigned to the East Siberian Arctic Shelf source in our BASE scenario (-55 ‰). Therefore is it possible that East Siberian Arctic Shelf emissions of 17 Tg yr^{-1} with a δ^{13}C value of -55 ‰ could be accommodated in model simulations of CH_4 and δ^{13}C-CH_4, provided substantial reductions in high latitude anthropogenic emissions of methane (for example ~33~~50~~ % across all sources) are also included in the simulations. In this case the agreement between the modelled and observed interpolar difference in CH_4 and δ^{13}C-CH_4, and the high northern latitude seasonal cycles of CH_4, δ^{13}C-CH_4 and δD-CH_4 could potentially be maintained. However, these scenarios could not be tested here as anthropogenic emissions were not tagged~~coloured~~ by latitude within the model. Emission totals for our BASE scenario and the BASE scenario including a 33% reduction to anthropogenic emissions >50°N, both give anthropogenic emission totals within the range of top-down and bottom-up emission estimates presented by Kirschke et al. (2013) (although towards the lower end for each source type when the 33% reduction is included). Although within current ranges of uncertainty, such large flux adjustments to high latitude anthropogenic sources would indicate the presence of important errors in current inventories of high latitude emissions.~~Such large flux adjustments to high latitude anthropogenic sources would indicate the presence of major systematic errors in the current inventories of high latitude emissions.~~

In summary, to accommodate an ESAS source of ~17 Tg yr^{-1} in our model simulations requires a substantial revision of our emission scenario in high northern latitudes. We require either:

(a) A reduction in wetland emissions north of 50° N of ~40 % (i.e. totalling ~18 Tg yr^{-1}, a number just below the minimum of a range of process model studies), and ESAS emissions to have a seasonality and highly depleted isotopic signature similar to high northern latitude wetlands (i.e. peaking during the summer ice-free period).

(b) A reassessment of anthropogenic methane emission inventories in which total emissions above 50° N are reduced by approximately ~~50~~33 %, and ESAS emissions are emitted approximately constantly through the year with an isotopic signature close to anthropogenic emissions (~55 ‰)

(c) A combination of the above

(d) The inclusion of an additional, as yet unrepresented, high latitude sink, such as the boreal plant sink outlined in Sundqvist et al. (2012).

7 Implications for Arctic sources

Model studies disagree over the magnitude and seasonal distribution of high northern latitude wetland methane emissions (Melton et al., 2013; Bohn et al. 2015). This disagreement needs to be resolved in order to better predict future wetland emissions in a warming climate. In this study, we find that high northern latitude wetland emissions have an important influence on both the magnitude and phase of high northern latitude seasonal cycles of CH_4 mixing ratios, $\delta^{13}C$-CH_4 and δD-CH_4. To date, measurements of δD source signatures are more limited than for $\delta^{13}C$, and uncertainties in source δD and $KIE^{H/D}$ values limit the conclusions that can be drawn from measurement-model comparisons of atmospheric data. However, with improved data, our model study shows that atmospheric observations of δD-CH_4, as well as $\delta^{13}C$-CH_4 could provide an important constraint on current emissions from Arctic wetlands and inter-annual trends in this climate-sensitive source.

In our model simulations, the model's ability to capture the magnitude and observed seasonal cycles of CH_4 mixing ratios, $\delta^{13}C$-CH_4 and δD-CH_4 in high northern latitudes is much improved if the seasonal cycle of the Fung et al. (1991) wetland emissions is delayed by one month (i.e. the wetland emission season starts and finishes one month later than in the prescribed dataset). As modelled atmospheric seasonal cycles at measurement station locations showed little sensitivity to emissions from north Asia (predominantly Siberia), this result is applicable to North American and North European wetland emissions. How this is interpreted will depend on the time-resolution of the emission dataset (one month for Fung et al., (1991)), and the temporal method of implementation in the model. In p-TOMCAT, emissions are linearly interpolated in time from the centre-point of the month. However, with improved temporal resolution of emissions, perhaps a better agreement could be obtained without the need to delay the seasonal cycle.

Figure 1 shows a comparison of seasonal cycles in high northern latitude wetland emissions from Fung et al. (1991) compared to emission data from wetland process models obtained as part of the recent WETCHIMP model comparison (Melton et al. 2013) and the methane model inversion study of Bousquet et al. (2011). The resulting emission distribution from delaying the Fung et al. (1991) seasonal cycle by one month generally falls within the range of model uncertainties, with the phase and shape of the seasonal cycle (though not emission magnitude) most closely matching that of the LPJ-Bern model.~~ However, t~~The delayed start to the emissions in FUNG_DEL results in notably smaller emissions in May than predicted by the other studies, excluding the atmospheric inversion study of Bousquet et al. (2011). The Bousquet et al. (2011) study obtained significant year to year differences in high latitude springtime emissions during the 1993 to 2009 time period considered. For their 1994-2004 period, emissions during May were significantly higher than for the years 2005 onwards, where they were often negative (see Fig. 1). Low~~er May-time emissions than predicted~~ emissions in May could be a result of continued snow cover at high latitudes or high water levels during the melt season limiting the amount of CH_4 released to the atmosphere due to oxidation in the water column. In addition, spring increases in CH_4 uptake by oxic forest soils and/or the canopy could contribute towards lower net emissions from high latitudes in May (Sundqvist et al. 2012). p-TOMCAT also requires a larger autumnal isotopically 'light' methane source than predicted by most wetland models to capture observed seasonal cycles of CH_4, $\delta^{13}C$-CH_4 and δD-CH_4. This result is consistent with a recent study by Zona et al.,

(2016) measuring year-round wetland fluxes at an Arctic wetland site. They found large methane fluxes continuing throughout the ‘zero curtain’ period, where subsurface soil temperatures remain active at ~0°C before freezing around December time, partly due to the insulating effects of snow cover. Other possible contributions towards an additional, isotopically light, autumnal methane source include processes releasing methane during tundra freezing (Mastepanov et al. 2008).

Using current literature estimates for northern high latitude methane emissions, our study suggests an ESAS methane source in the lower half of published estimated ranges (0.5 to 17 Tg yr^{-1}). This is in agreement with the study by Berchet et al. (2016), which used synoptic data from long-term methane measurement sites to constrain ESAS emissions from 0.5 to 4.3 Tg yr^{-1}. We find that substantial adjustments in estimates of high latitude methane source flux magnitudes or isotopic source signatures are required in order to reconcile East Siberian Arctic Shelf emissions as large as 17 Tg yr^{-1} with global scale atmospheric observations of CH_4 and $\delta^{13}C$-CH_4. Depending on currently-~~-~~lacking information on the seasonality and isotopic signature of an ESAS source, these include reducing high northern latitude wetland emissions by ~40 % (to a value just below the minimum of a range of values predicted by process models), reducing high northern latitude emissions from anthropogenic emission inventories by ~33~~50~~ % or a combination of the two. Alternatively, a missing seasonal sink, such as the destruction of methane by boreal vegetation suggested by Sundqvist et al. (2012) could help reconcile large emissions from the ESAS with global scale atmospheric observations. Further information on the isotopic signature and seasonality of an ESAS source would be of benefit in distinguishing between possible scenarios.

Acknowledgements

The authors acknowledge funding from the NERC MAMM project (NE/I029161/1 and NE/I028874/1). NJW and JAP thank NCAS-Climate for funding. NJW and JAP also thank NERC for funding via the projects NE/K004964/1 and NE/I010750/1. DL, JF, REF and EGN thank NERC for funding via projects NE/K006045/1 and NE/I014683/1. This study was also supported by the ERC under the ACCI project, grant number 267760.

References

Allan, W., Struthers, H., and Lowe, D. C.: Methane carbon isotope effects caused by atomic chlorine in the marine boundary layer: Global model results compared with Southern Hemisphere measurements, J. Geophys. Res., 112, D04306, doi:10.1029/2006JD007369, 2007.

Bekki, S., and Pyle, J. A., A two-dimensional modeling study of the volcanic eruption of Mount Pinatubo, J. Geophys. Res., 99(D9), 18861–18869, doi:10.1029/94JD00667, 1994.

Bergamaschi, P., Bräunlich, M., Marik, T., and Brenninkmeijer, C. A. M.: Measurements of the carbon and hydrogen isotopes of atmospheric methane at Izaña, Tenerife: Seasonal cycles and synoptic-scale variations, J. Geophys. Res., 105(D11), 14531–14546, doi:10.1029/1999JD901176, 2000.

Bergamaschi, P., Houweling, S., Segers, A., Krol, M., Frankenburg, C., Scheepmaker, R. A., Dlugokencky, E., Wofsy, S. C., Kort, E. A., Sweeney, C., Schuck, T., Brenninkmeijer, Chen, H., Beck, V. and Gerbig, C.: Atmospheric methane in the first decade of the 21st Century: Inverse modelling analysis using SCIAMACHY satellite retrievals and NOAA surface measurements, J. Geophys. Res., 118, 7350-7369, doi:10.1002/jgrd.50480, 2013.

Berchet, A., Bousquet, P., Pison, I., Locatelli, R., Chevallier, F., Paris, J.-D., Dlugokencky, E. J., Laurila, T., Hatakka, J., Viisanen, Y., Worthy, D. E. J., Nisbet, E. G., Fisher, R. E., France, J. L., Lowry, D., Ivakhov, V., and Hermansen, O.: Atmospheric constraints on the methane emissions from the East Siberian Shelf, Atmos. Chem. Phys., 16, 4147-4157, doi:10.5194/acp-16-4147-2016, 2016.

Bilek, R. S., Tyler, S. C., Kurihara, M. and Yagi, K.: Investigation of cattle methane production and emission over a 24-hour period using measurements of δ13C and δD of emitted CH4 and rumen water, J. Geophys. Res., 106(D14), 15405–15413, doi:10.1029/2001JD900177, 2001.

Bohn, T. J., Melton, J. R., Ito, A., Kleinen, T., Spahni, R., Stocker, B. D., Zhang, B., Zhu, X., Schroeder, R., Glagolev, M. V., Maksyutov, S., Brovkin, V., Chen, G., Denisov, S. N., Eliseev, A. V., Gallego-Sala, A., McDonald, K. C., Rawlins, M.A., Riley, W. J., Subin, Z. M., Tian, H., Zhuang, Q., Kaplan, J. O.: WETCHIMP-WSL: intercomparison of wetland methane emissions models over West Siberia, Biogeosciences, 12, 3321—3349, doi:10.5194/bg-12-3321-2015, 2015.

Born, M., Dörr, H. and Levin, I: Methane consumption in aerated soils of the temperate zone. Tellus B, 42, 2–8, doi: 10.1034/j.1600-0889.1990.00002.x, 1990.

Bousquet, P., Ringeval, B., Pison, I., Dlugokencky, E. J., Brunke, E.-G., Carouge, C., Chevallier, F., Fortems-Cheiney, A., Frankenberg, C., Hauglustaine, D. A., Krummel, P. B., Langenfelds, R., L. , Ramonet, M., Schmidt, M., Steele, L. P., Szopa, S., Yver, C., Viovy, N. and Ciais, P.: Source attribution of the changes in atmospheric methane for 2006–2008, Atmos. Chem. Phys., 11, 3689–3700, doi:10.5194/acp-11-3689-2011, 2011.

Christensen, T. R., Ekberg, A., Ström, L., Mastepanov, M., Panikov, N., Öquist, M., Svensson, B. H., Nykänen, H., Martikainen, P. J., and Oskarsson, H., Factors controlling large scale variations in methane emissions from wetlands, Geophys. Res. Lett., 30, 1414, doi:10.1029/2002GL016848, 2003.

Christensen, T. R., Johansson, T., Akerman, H. J. and Mastepanov, M.: Thawing sub-arctic permafrost: effects on vegetation and methane emissions, Geophys. Res. Lett., 31, L04501, 2004.

Cicerone, R. J., and Oremland, R. S., Biogeochemical aspects of atmospheric methane, Global Biogeochemical Cycles, 2, 299-327, doi:10.1029/GB002i004p00299, 1988.

Cook, P. A., Savage, N. H., Turquety, S., Carver, G. D., O'Connor, F. M., Heckel, A., Stewart, D., Whalley, L. K., Parker, A. E., Schlager, H., Singh, H. B., Avery, M. A., Sachse, G. W., Brune, W., Richter, A., Burrows, J. P., Purvis, R., Lewis, A. C., Reeves, C. E., Monks, P. S., Levine, J.G. and Pyle, J. A.: Forest fire plumes over the North Atlantic: p-TOMCAT model simulations with aircraft and satellite measurements from the ITOP/ICARTT campaign, J. Geophys. Res., 112, D10S43, doi:10.1029/2006JD007563, 2007.

Craig, H., Isotope standards for carbon and oxygen and correction factors for mass-spectrometric analysis of carbon dioxide, Geochirn. Cosrnochirn. Acta, 12, 133-149, 1957.

DeMore, W. B., Rate constant ratio for the reaction of OH with CH3D and CH4, J. Phys. Chem., 97, 8564–8566, 1993.

DeWit, J.C., Van der Straaten, C.M. and Mook, W.G.: Determination of the absolute hydrogen isotopic ratio of V-SMOW and SLAP, Geostand. Newsl., 4, (1), 33-36, 1980.

Dlugokencky, E. J., Steele, L. P., Lang, P. M., and Masarie, K. A.: Atmospheric methane at Mauna Loa and Barrow observatories: Presentation and analysis of in situ measurements, J. Geophys. Res., 100(D11), 23103–23113, doi:10.1029/95JD02460, 1995.

Dlugokencky, E. J., Masarie, K. A., Lang, P. M. and Tans, P. P.: Continuing decline in the growth rate of atmospheric methane, Nature, 393, 447-450, doi:10.1038/30934, 1998.

Dlugokencky, E. J., Nisbet, E. G., Fisher, R., and Lowry, D.: Global atmospheric methane: budget, changes and dangers, Phil. Trans. R. Soc. A, 369, 2058-2072; doi: 10.1098/rsta.2010.0341, 2011.

Dlugokencky, E.J., Lang, P. M., Crotwell, A. M., Masarie, K. A. and Crotwell, M. J.: Atmospheric Methane Dry Air Mole Fractions from the NOAA ESRL Carbon Cycle Cooperative Global Air Sampling Network, 1983-2012, Version: 2013-08-28, Path: ftp://aftp.cmdl.noaa.gov/data/trace_gases/ch4/flask/surface/, 2013.

Fisher, R. E., Sriskantharajah, S., Lowry, D. , Lanoisellé, M., Fowler, C. M. R., James, R. H., Hermansen, O., Lund Myhre, C., Stohl, A., Greinert, J., Nisbet-Jones, P. B. R., Mienert, J., Nisbet, E. G.: Arctic methane sources: Isotopic evidence for atmospheric inputs, Geophys. Res. Lett., 38, L21803, doi:10.1029/2011GL049319, 2011.

Fung, I., John, J., Lerner, J., Matthews, E., Prather, M., Steele, L. P., and Fraser, P. J.: Three-dimensional model synthesis of the global methane cycle, J. Geophys. Res., 96, 13033-13065, doi:10.1029/91JD01247, 1991.

Gierczak, T., Talukdar, R. K., Herndon, S. C., Vaghjiani, G. L., and Ravishankara, A. R.: Rate Coefficients for the Reactions of Hydroxyl Radicals with Methane and Deuterated Methanes, The Journal of Physical Chemistry, 101 (17), 3125-3134, doi: 10.1021/jp963892r, 1997.

Graves, C. A., Steinle, L., Rehder, G., Niemann, H., Connelly, D. P., Lowry, D., Fisher, R. E., Stott, A. W., Sahling, H., and James, R. H., Fluxes and fate of dissolved methane released at the seafloor at the landward limit of the gas hydrate stability zone offshore western Svalbard, J. Geophys. Res. Oceans, 120, 6185–6201, doi:10.1002/2015JC011084, 2015.

Gupta, M., Tyler, S., and Cicerone, R.: Modeling atmospheric $\delta^{13}CH_4$ and the causes of recent changes in atmospheric CH_4 amounts, J. Geophys. Res., 101(D17), 22923–22932, doi:10.1029/96JD02386, 1996.

Hausmann, P., Sussmann, R., and Smale, D.: Contribution of oil and natural gas production to renewed increase in atmospheric methane (2007–2014): top–down estimate from ethane and methane column observations, Atmos. Chem. Phys., 16, 3227-3244, doi:10.5194/acp-16-3227-2016, 2016.

Houweling, S., Dentener, F., Lelieveld, J., Walter, B., and Dlugokencky, E.: The modeling of tropospheric methane: How well can point measurements be reproduced by a global model?, J. Geophys. Res., 105, 8981-9002, doi:10.1029/1999JD901149, 2000.

Kort, E. A., Wofsy, S. C., Daube, B. C., Diao, M., Elkins, J. W., Gao, R. S., Hintsa, E. J., Hurst, D. F., Jimenez, R., Moore, F. L., Spackman, J. R. and Zondlo, M. A.: Atmospheric observations of Arctic Ocean methane emissions up to 82° north, Nature Geoscience 5, 318–32, doi:10.1038/ngeo1452, 2012.

Kuhlmann, A. J., Worthy, D. E. J., Trivett, N. B. A. and Levin, I.: Methane emissions from a wetland region within the Hudson Bay Lowland: An atmospheric approach, J. Geophys. Res., 103(D13), 16009–16016, doi:10.1029/98JD01024, 1998.

Lawler, M. J., Sander, R., Carpenter, L. J., Lee, J. D., von Glasow, R., Sommariva, R., and Saltzman, E. S.: HOCl and Cl2 observations in marine air, Atmos. Chem. Phys., 11, 7617-7628, doi:10.5194/acp-11-7617-2011, 2011.

Levin, I., Bergamaschi, P., Dörr, H., Trapp, D.: Stable isotopic signature of methane from major sources in Germany, Chemosphere, 26, 161-177, 1993.

Mastepanov, M., Sigsgaard, C., Dlugokencky, E. G., Houweling, S., Ström, L., Tamstorf, M. P. and Christensen, T. R.: Large tundra methane burst during onset of freezing, Nature, 456, 628-630, doi:10.1038/nature07464, 2008.

Melton, J. R., Wania, R., Hodson, E. L., Poulter, B., Ringeval, B., Spahni, R., Bohn, T., Avis, C. A., Beerling, D. J., Chen, G., Eliseev, A. V., Denisov, S. N., Hopcroft, P. O., Lettenmaier, D. P., Riley, W. J., Singarayer, J. S., Subin, Z. M., Tian, H., Zurcher, S., Brovkin, V., van Bodegom, P. M., Kleinen, T., Yu, Z. C., and Kaplan, J. O.: Present state of global wetland extent and wetland methane modelling: conclusions from a model inter-comparison project (WETCHIMP), Biogeosciences, 10, 753–788, doi:10.5194/bg-10-753-2013, 2013.

Milkov, A. V., Molecular and stable isotope compositions of natural gas hydrates: A revised global dataset and basic interpretations in the context of geological settings, Org. Geochem., 36(5), 681-702, doi:10.1016/j.orggeochem.2005.01.010, 2005.

Miller, J. B., K. A. Mack, R. Dissly, J. W. C. White, E. J. Dlugokencky, and P. P. Tans, Development of analytical methods and measurements of 13C/12C in atmospheric CH4 from the NOAA Climate Monitoring and Diagnostics Laboratory Global Air Sampling Network, J. Geophys. Res., 107(D13), doi:10.1029/2001JD000630, 2002.

Nakagawa, F., Yoshida, N., Nojiri, Y., Makarov, V. N.: Production of methane from alasses in eastern Siberia: Implications from its 14C and stable isotopic compositions, Global Biogeochem. Cycles, 16(3), doi:10.1029/2000GB001384, 2002.

Nakagawa, F., Yoshida, N., Sugimoto, A., Wada, E., Yoshioka, T., Ueda, S. and Vijarnsorn, P.: Stable Isotope and Radiocarbon Compositions of Methane Emitted from Tropical Rice Paddies and Swamps in Southern Thailand, Biogeochemistry, 61, 1-19, 2002b.

Nisbet, E. G., Dlugokencky, E. J., Bousquet, P.: Methane on the rise again, Science, 343, 493-495. doi:10.1126/science.1247828, 2014.

Nisbet, E.G., Dlugokencky, E. J., Manning, M. R., Lowry, D., Fisher, R. E., France, J. L., Michel, S. E., Miller, J. B., White, J. W. C., Vaughn, B., Bousquet, P., Pyle, J. A., Warwick, N. J., Cain, M., Brownlow, R., Zazzeri, G., Lanoisellé, M., Manning, A. C., Gloor, E., Worthy, D. E. J., Brunke, E.-G., Labuschagne, C., Wolff, E. W. and Ganesan, A. L., Rising atmospheric methane: 2007-2014 growth and isotopic shift,~~—~~ Global Biogeochem. Cyc., 30, 1356-1370, doi:10.1002/2016GB005406, 2016.l~~submitted to Global. Biogeochem. Cyc~~..

O'Shea, S. J., Allen, G., Gallagher, M. W., Bower, K., Illingworth, S. M., Muller, J. B. A., Jones, B. T., Percival, C. J., Bauguitte, S. J-B., Cain, M., Warwick, N., Quiquet, A., Skiba, U., Drewer, J., Dinsmore, K., Nisbet, E. G., Lowry, D., Fisher, R. E., France, J. L., Aurela, M., Lohila, A., Hayman, G., George, C. , Clark, D. B., Manning, A. J., Friend, A. D. and Pyle, J., Methane and carbon dioxide fluxes and their regional scalability for the European Arctic wetlands during the MAMM project in summer 2012, Atmos. Chem. Phys., 14, 13159-13174, doi: 10.5194/acp-14-13159-2014, 2014.

Pelletier, L., T. R. Moore, N. T. Roulet, M. Garneau, and V. Beaulieu-Audy, Methane fluxes from three peatlands in the La Grande Riviere watershed, James Bay lowland, Canada, J. Geophys. Res., 112, G01018, doi:10.1029/2006JG000216, 2007.

Petrescu, A. M. R., van Beek, L. P. H., van Huissteden, J., Prigent, C., Sachs, T., Corradi, C. A. R., Parmentier, F. J. W., and Dolman, A. J.: Modeling regional to global CH$_4$ emissions of boreal and arctic wetlands, Global Biogeochem. Cycles, 24, GB4009, doi:10.1029/2009GB003610, 2010.

Pickett-Heaps, C. A., Jacob, D. J., Wecht, K. J., Kort, E. A., Wofsy, S. C., Diskin, G. S., Worthy, D. E. J., Kaplan, J. O., Bey, I. and Drevet, J.: Magnitude and seasonality of wetland methane emissions from the Hudson Bay Lowlands (Canada), Atmos. Chem. Phys., 11, 3773–3779, doi:10.5194/acp-11-3773-2011, 2011.

Quay, P., Stutsman, J., Wilbur, D., Snover, A., Dlugokencky, E. J., Brown, T., The isotopic composition of atmospheric methane, Global Biogeochem. Cycles, 13(2), 445–461, doi:10.1029/1998GB900006, 1999.

Reshetnikov, A. I., Paramonova, N. N. and Shashkov, A. A.: An evaluation of historical methane emissions from the Soviet gas industry, J. Geophys. Res., 105(D3), 3517–3529, doi:10.1029/1999JD900761, 2000.

Rigby, M., Manning, A. J., and Prinn, R. G.: The value of high-frequency, high-precision methane isotopologue measurements for source and sink estimation, J. Geophys. Res., 117, D12312, doi:10.1029/2011JD017384, 2012.

Saueressig, G., Crowley, J. N., Bergamaschi, P., Brühl, C., Brenninkmeijer, C. A. M. and Fischer, H.: Carbon 13 and D kinetic isotope effects in the reactions of CH4 with O(1 D) and OH: New laboratory measurements and their implications for the isotopic composition of stratospheric methane, J. Geophys. Res., 106(D19), 23127–23138, doi:10.1029/2000JD000120, 2001.

Saunois, M., Bousquet, P., Poulter, B., Peregon, A., Ciais, P., Canadell, J. G., Dlugokencky, E. J., Etiope, G., Bastviken, D., Houweling, S., Janssens-Maenhout, G., Tubiello, F. N., Castaldi, S., Jackson, R. B., Alexe, M., Arora, V. K., Beerling, D. J., Bergamaschi, P., Blake, D. R., Brailsford, G., Brovkin, V., Bruhwiler, L., Crevoisier, C., Crill, P., Curry, C., Frankenberg, C., Gedney, N., Höglund-Isaksson, L., Ishizawa, M., Ito, A., Joos, F., Kim, H.-S., Kleinen, T., Krummel, P., Lamarque, J.-F., Langenfelds, R., Locatelli, R., Machida, T., Maksyutov, S., McDonald, K. C., Marshall, J., Melton, J. R., Morino, I., O'Doherty, S., Parmentier, F.-J. W., Patra, P. K., Peng, C., Peng, S., Peters, G. P., Pison, I., Prigent, C., Prinn, R., Ramonet, M., Riley, W. J., Saito, M., Schroeder, R., Simpson, I. J., Spahni, R., Steele, P., Takizawa, A., Thornton, B. F., Tian, H., Tohjima, Y., Viovy, N., Voulgarakis, A., van Weele, M., van der Werf, G., Weiss, R., Wiedinmyer, C., Wilton, D. J., Wiltshire, A., Worthy, D., Wunch, D. B., Xu, X., Yoshida, Y., Zhang, B., Zhang, Z., and Zhu, Q.: The Global Methane Budget: 2000–2012, Earth Syst. Sci. Data Discuss., doi:10.5194/essd-2016-25, 2016.

Schaefer, H., Mikaloff Fletcher, S. E., Veidt, C., Lassey, K. R., Brailsford, G. W., Bromley, T. M., Dlugokencky, E. J., Englund Michel, S., Miller, J. B., Levin, I., Lowe, D. C., Martin, R. J., Vaughn, B. H., White, J. W. C.: A 21st-century shift from fossil-fuel to biogenic methane emissions indicated by $^{13}CH_4$, Science, 352, 80-84, doi: 10.1126/science.aad2705, 2016.

Schoell. M.: The hydrogen and carbon isotopic composition of methane from natural gases of various origins, Geochimica et Cosmochimica Acta, 44, 649-661, 1980.

Shakhova, N., Semiletov, I., Salyuk, A., Yusupov, V., Kosmach, D., Gustafsson, Ö., Extensive methane venting to the atmosphere from sediments of the East Siberian Arctic Shelf, Science, 327, 1246-1250, doi:10.1126/science.1182221, 2010.

Shakhova, N., Semiletov, I., Leifer, I., Sergienko, V., Salyuk, A., Kosmach, D., Chernykh, D., Stubbs, C., Nicolsky, D., Tumskoy, V. and Gustafsson, Ö.: Ebullition and storm-induced methane release from the East Siberian Arctic Shelf, Nature Geoscience, 7, 64–70, doi:10.1038/ngeo2007, 2014.

Snover, A. K., Quay, P. D., and Hao, W. M.: The D/H content of methane emitted from biomass burning, Global Biogeochem. Cycles, 14(1), 11–24, doi:10.1029/1999GB900075, 2000.

Song, C., Xu, X., Sun, X., Tian, H., Sun, L., Miao, Y., Wang, X. and Guo, Y.: Large methane emission upon spring thaw from natural wetlands in the northern permafrost region, Environ. Res. Lett. 7 034009, doi:10.1088/1748-9326/7/3/034009, 2012.

Spivakovsky, C. M., et al.: Three-dimensional climatological distribution of tropospheric OH: Update and evaluation, J. Geophys. Res., 105(D7), 8931–8980, doi:10.1029/1999JD901006, 2000.

Sriskantharajah, S., Fisher, R. E., Lowry, D., Aalto, T., Hatakka, J., Aurela, M., Laurila, T., Lohila, A., Kuitunen, E. and Nisbet, E. G., Tellus B, 64, 18818, http://dx.doi.org/10.3402/tellusb.v64i0.18818, 2012.

Sundqvist, E., Crill, P., Mölder, M., Vestin, P., and Lindroth, A.: Atmospheric methane removal by boreal plants, Geophys. Res. Lett., 39, L21806, doi:10.1029/2012GL053592, 2012.

Tan, Z. and Zhuang, Q.: Arctic lakes are continuous methane sources to the atmosphere under global warming, Environ. Res. Lett., 10, 054016, doi:10.1088/1748-9326/10/5/054016, 2015.

Tyler, S. C., Zimmerman, P. R., Cumberbatch, C., Greenberg, J. P., Westberg, C., and Darlington, J. P. E. C.: Measurements and interpretation of $\delta^{13}C$ of methane from termites, rice paddies, and wetlands in Kenya, Global Biogeochem. Cycles, 2, 341–355, doi:10.1029/GB002i004p00341, 1988.

Tyler, S. C., Rice, A. L. and Ajie, H. O.: Stable isotope ratios in atmospheric CH4: Implications for seasonal sources and sinks, J. Geophys. Res., 112, D03303, doi:10.1029/2006JD007231, 2007.

Umezawa, T., Machida, T., Ishijima, K., Matsueda, H., Sawa, Y., Patra, P. K., Aoki, S. and Nakazawa, T.: Carbon and hydrogen isotopic ratios of atmospheric methane in the upper troposphere over the Western Pacific, Atmos. Chem. Phys., 12, 8095-8113, doi:10.5194/acp-12-8095-2012, 2012.

Van der Werf, G. R., Randerson, J. T., Giglio, L., Collatz, G. J., Kasibhatla, P. S., and Arellano, Jr., A. F.: Interannual variability in global biomass burning emissions from 1997 to 2004, Atmos. Chem. Phys., 6, 3423–3441, 2006.

Vaular, E. N., Barth, T., and Haflidason, H., The geochemical characteristics of the hydrate-bound gases from the Nyegga pockmark field, Norwegian Sea, Org. Geochem., 41(5), 437-444, doi:10.1016/j.orggeochem.2010.02.005, 2010.

Waldron, S., Lansdown, J. M., Scot, E. M., Fallick, A. E., and Hall, A.. J.: The global influence of the hydrogen isotope composition of water on that of bacteriogenic methane from shallow freshwater environments, Geochimica et Cosmochimica Acta**,** 63, 2237-2245**,** doi:10.1016/S0016-7037(99)00192-1**,** 1999.

Wang, J. S., Logan, J. A., McElroy, M. B., Duncan, B. N., Megretskaia, I. A., and R. M. Yantosca, R. M.: A 3-D model analysis of the slowdown and interannual variability in the methane growth rate from 1988 to 1997, Global Biogeochem. Cycles, 18, GB3011, doi:10.1029/2003GB002180, 2004.

Warwick, N. J., Pyle, J. A., Carver, G. D., Yang, X., Savage, N. H., O'Connor, F. M., and Cox, R. A.: Global modeling of biogenic bromocarbons, J. Geophys. Res., 111, D24305, doi:10.1029/2006JD007264, 2006.

Warwick, N. J., Archibald, A. T., Ashworth, K., Dorsey, J., Edwards, P. M., Heard, D. E., Langford, B., Lee, J., Misztal, P. K., Whalley, L. K., and Pyle, J. A.: A global model study of the impact of land-use change in Borneo on atmospheric composition, Atmos. Chem. Phys., 13, 9183-9194, doi:10.5194/acp-13-9183-2013, 2013.

White, J.W.C. and Vaughn, B. H.: University of Colorado, Institute of Arctic and Alpine Research (INSTAAR), Stable Isotopic Composition of Atmospheric Methane (13C) from the NOAA ESRL Carbon Cycle Cooperative Global Air Sampling Network, 1998-2014, Version: 2015-08-03, path: ftp://aftp.cmdl.noaa.gov/data/trace_gases/ch4c13/flask/, 2015.

White, J. W. C., Vaughn, B. H., and Michel, S. E.: University of Colorado, Institute of Arctic and Alpine Research (INSTAAR), Stable Isotopic Composition of Atmospheric Methane (D/H) from the NOAA ESRL Carbon Cycle Cooperative Global Air Sampling Network, 2005-2009, Version: 2016-04-26, Path: ftp://aftp.cmdl.noaa.gov/data/trace_gases/ch4h2/flask/, 2016.

Whiticar, M. and Schaefer, H.: Constraining past global tropospheric methane budgets with carbon and hydrogen isotope ratios in ice, Philos. Trans. R. Soc. A, 365, 1793-1828, 2007.

Worthy, D. E. J., Chan, E., Ishizawa, M., Chan, D., Poss, C., Dlugokencky, E. J., Maksyutov, S., and Levin, I.: Decreasing anthropogenic methane emissions in Europe and Siberia inferred from continuous carbon dioxide and methane observations at Alert, Canada, J. Geophys. Res., 114, D10301, doi:10.1029/2008JD011239, 2009.

Yamada, K., Yoshidaa, N., Nakagawa, F., Inoue, G., Source evaluation of atmospheric methane over western Siberia using double stable isotopic signatures, Organic Geochemistry, 36, 717–726, doi:10.1016/j.orggeochem.2005.01.016, 2005.

Zazzeri, G., Lowry, D., Fisher, R. E., France, J. L., Lanoisellé, M. and Nisbet E. G., Plume mapping and isotopic characterisation of anthropogenic methane sources, Atmos. Environ. 110, 151-162, doi:10.1016/j.atmosenv.2015.03.029, 2015.

Zona, D., Gioli, B., Commane, R., Lindaas, J., Wofsy, S. C., Miller, C. E., Dinardo, S. J., Dengel, S., Sweeney, C., Karion, A., Chang, R. Y.-W., Henderson, J. M., Murphy, P. C., Goodrich, J. P., Moreaux, V., Liljedahl, A., Watts, J. D., Kimball, J.

S., Lipson, D. A., and Oechel, W. C., Cold season emissions dominate the Arctic tundra methane budget, Proc. Natl. Acad. Sci., 113, 40-45, doi: 10.1073/pnas.1516017113, 2016.

Table 1. Global methane source magnitudes and isotopic signatures used in p-TOMCAT

Surface Source/Sink	Global flux (Tg/yr)	High latitude (>50°N) flux (Tg/yr)	δ^{13}C-CH$_4$ (‰)	δD-CH$_4$ (‰)
Northern Wetlands	30[1]	30.0	-70[d,h,l,n*]	-360[f,n*]
Tropical Wetlands	200[1]	0.0	-55[b,m*]	-320[g,o*]
Hydrates	5[1]	5.0	-55[d*]	-190[p]
Coal	40[2,3]	3.2	-50[i,q*]	-140[p]
Gas	63[2,3]	15.3	-40[b,n*]	-185[i,j,n*]
Biomass burning	31[4]	3.1	-26[b]	-210[k]
Ruminants	110[2]	8.0	-63[a,c*]	-360[a*]
Landfills	27[2]	4.6	-53[b]	-310[i,p]
Sewage	29[2]	1.8	-57[b]	-310[r]
Rice	33[2]	0.0	-62[b,g,m*]	-330[p*]
Termites	20[1]	1.1	-57[e,m*]	-390[p]
Total	588	72.1		

The geographical and seasonal distribution of methane flux data is based on [1]Fung et al., 1991, [2]EDGAR v4.1 (http://edgar.jrc.ec.europa.eu/overview.php?v=41) for 2005, [3]Gurney et al., 2005, and [4]Van der Werf et al., 2006. Source isotopic signature data are based on reported values from: [a]Bilek et al., 2001, [b]Dlugokencky et al., 2011, [c]Levin et al., 1993, [d]Fisher et al., 2011, [e]Gupta et al., 1996, [f]Nakagawa et al., 2002a, [g]Nakagawa et al., 2002b, [h]O'Shea et al., 2014, [i]Quay et al., 1999, [j]Schoell, 1980, [k]Snover et al., 2000, [l]Sriskantharajah et al., 2012, [m]Tyler et al., 1988, [n]Umezawa et al., 2012, [o]Waldron et al., 1999, [p]Whiticar and Schaefer, 2007 , [q]Zazzeri et al., 2015, [r]value used taken from landfill data, *value is within a range of quoted literature estimates.

Table 2.

Scenario	Difference from BASE Scenario
BASE	-
DEC_KIE	$KIE^{(CH4+OH)}/KIE^{(CH3D+OH)}$ is decreased from 1.29 to 1.16[a]
WETLD_δD	δD signature for wetland emissions >50°N changed to -500‰
NO_WETLD	Wetland emissions >50°N removed
INC_WETLD	Wetland emissions >50°N increased by 50% to 45 Tg/yr
DEL_WET	Seasonal cycle of wetland emissions >50°N delayed by one month throughout the year
NO_HYD	Hydrate emissions removed
INC_HYD	Hydrate emissions increased to 17 Tg/yr
WET_HYD	Hydrate emissions increased to 17 Tg/yr and wetland emissions decreased to 18 Tg/yr
WET_HYD_δ13C	As WET_HYD, except isotopic signature for ESAS emissions is changed to -70 ‰

[a] See Table S1.

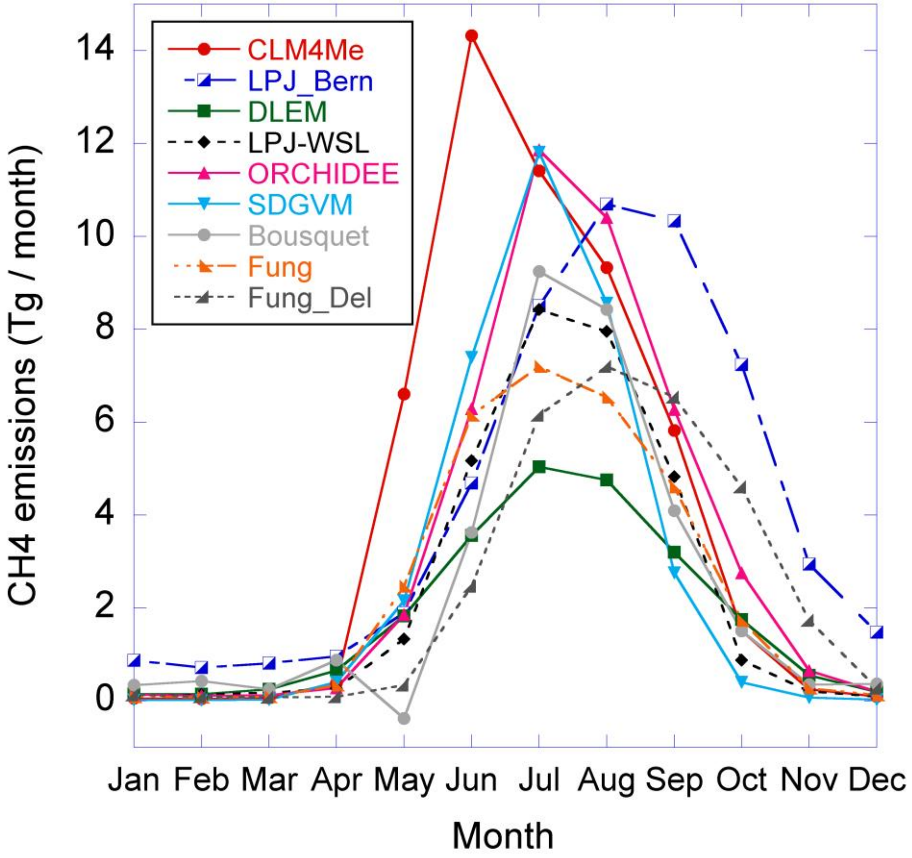

Figure 1: A comparison of seasonal cycles in northern wetland emissions (>50° N) from Fung et al. (1991) (Fung), Fung et al. (1991) with a seasonal cycle delayed by one month (Fung_Del), mean annual emission data for 1993-2004 from wetland process models obtained as part of the recent WETCHIMP model comparison (CLM4Me, LPJ_Bern, DLEM, WSL, ORCHIDEE, SDGVM; Melton et al., 2013) and mean annual emission data for ~~1993-2004~~2005-2009 from the methane model inversion study of Bousquet et al., (2011).

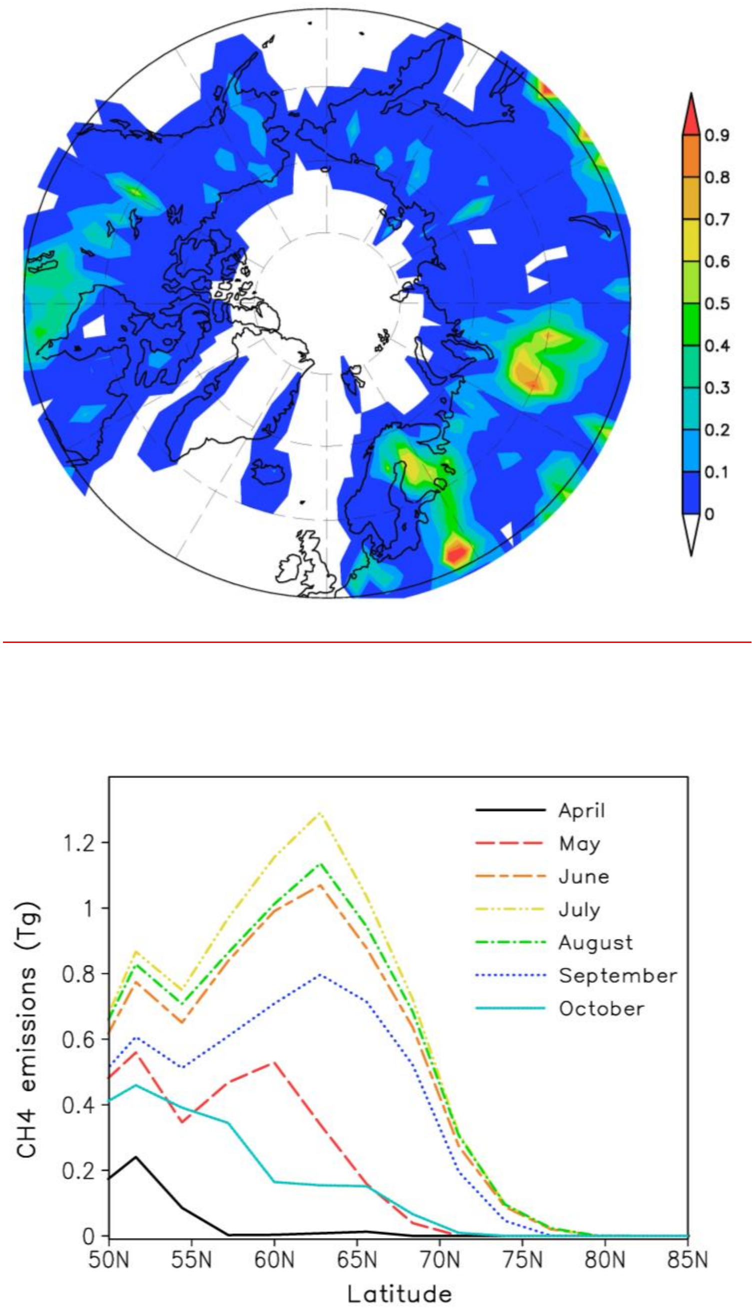

Figure 2: a) The geographical distribution of annual mean wetland emissions (mg/m^2/hr) above 50° N used in the model simulations. b) Zonally summed monthly CH_4 emissions from a) for April to September. Emissions in a) and b) have been interpolated to the model resolution (~2.8° x 2.8°)~~Emissions~~ and are based on Fung et al., 1991.

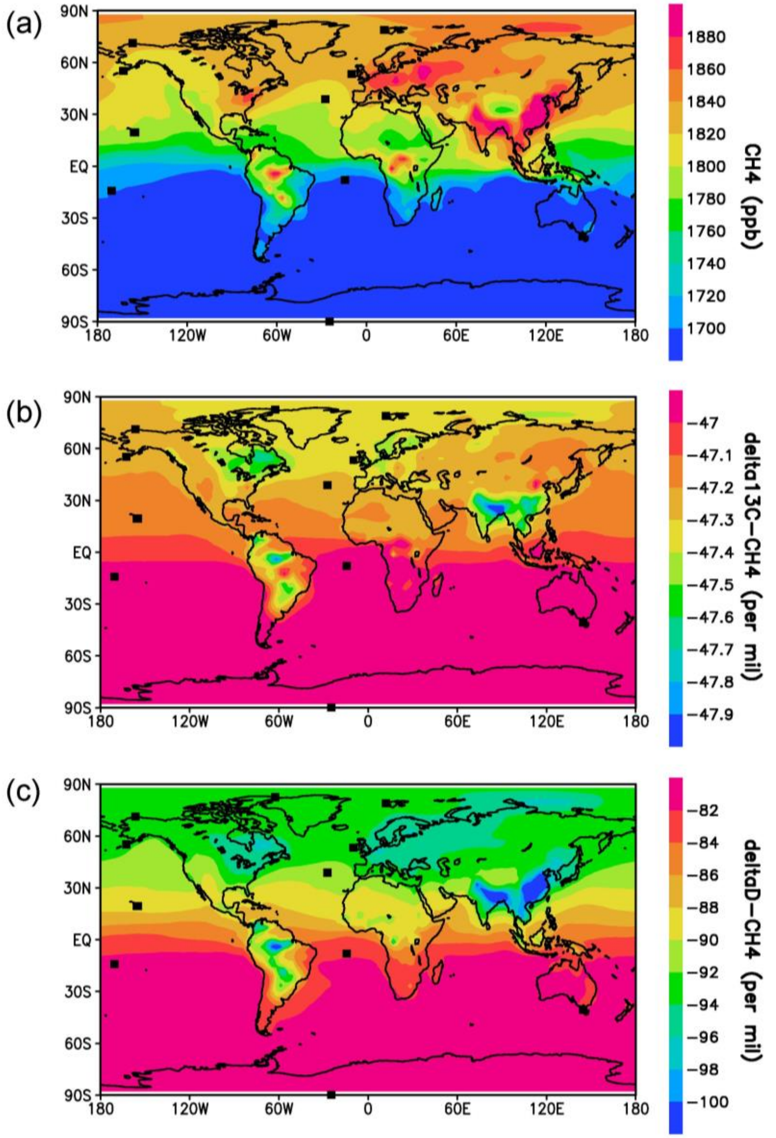

Figure 3: Modelled global annual mean surface distributions of (a) CH$_4$, (b) δ^{13}C-CH$_4$ and (c)δD-CH$_4$ for the p-TOMCAT BASE scenario. Locations of measurement data sites used in this study are marked as black squares.

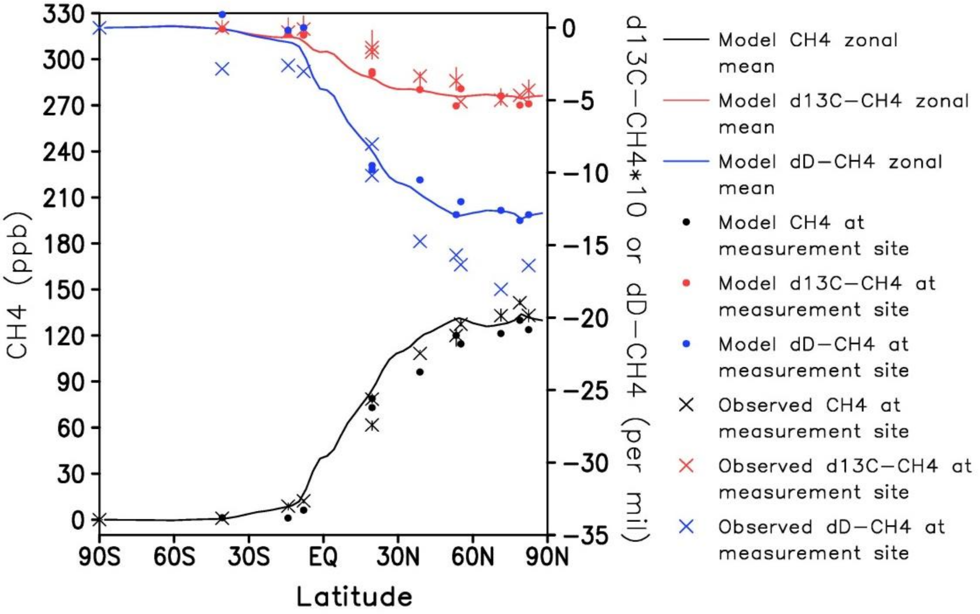

Figure 4: The difference between surface annual mean CH$_4$, δ^{13}C-CH$_4$ and δD-CH$_4$ and South Pole annual mean values for CH$_4$, δ^{13}C-CH$_4$ and δD-CH$_4$. Results from the p-TOMCAT BASE scenario (including sampling the model at station locations) are compared to NOAA-ESRL and CU-INSTAAR observations. Where there are sufficient data available in the 2005 to 2009 period, the range in annual mean station-South Pole observed differences is represented by a vertical bar. CH$_4$ mixing ratios are shown in black, δ^{13}C-CH$_4$ in red and δD-CH$_4$ in blue. Variations in δ^{13}C-CH$_4$ have been multiplied by a factor of 10.

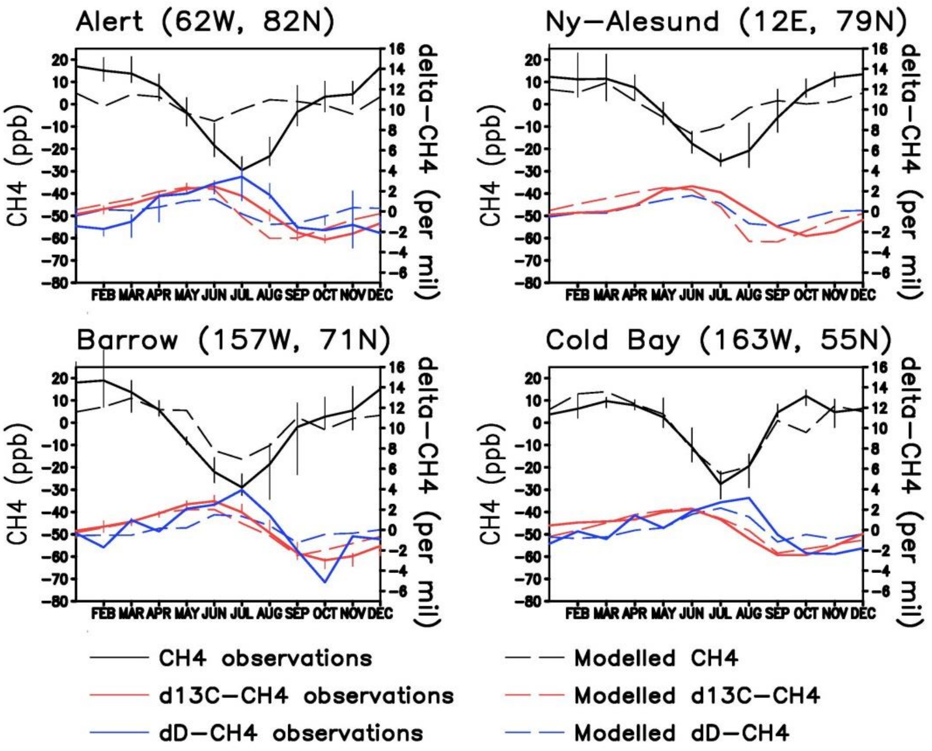

Figure 5: A comparison of modelled seasonal cycles of CH_4, $\delta^{13}C$-CH_4 and δD-CH_4 from the p-TOMCAT BASE scenario and NOAA-ESRL and CU-INSTAAR observations (δD-CH_4 is not plotted for Ny-Alesund due to insufficient data). Annual means have been subtracted from both the model and measurement data. Variations in $\delta^{13}C$-CH_4 have been multiplied by a factor of 10. Where there are sufficient data available in the 2005 to 2009 period, the range of observed monthly mean values relative to the annual mean is represented by a vertical bar.

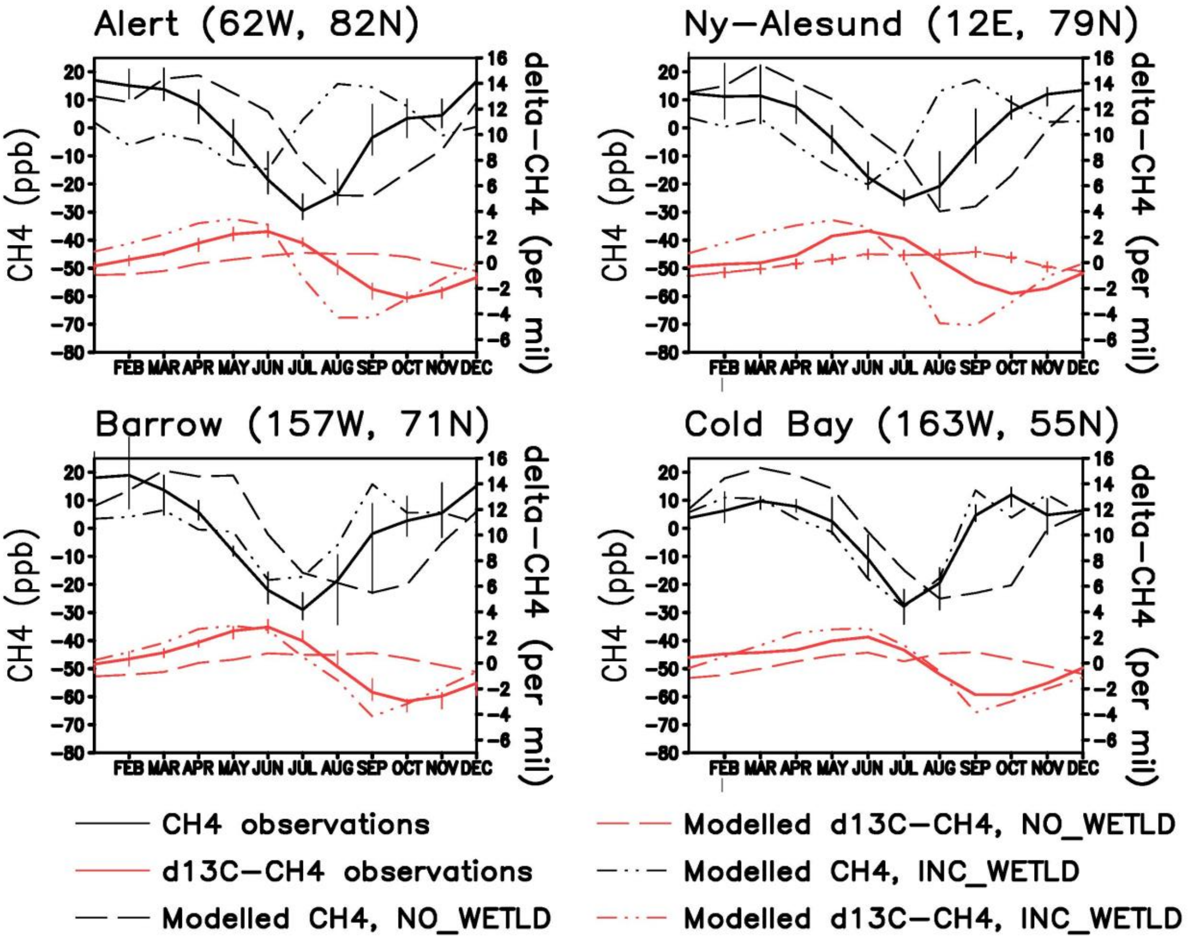

Figure 6: Modelled seasonal cycles of CH_4 and $\delta^{13}C$-CH_4 compared to NOAA-ESRL and CU-INSTAAR observations. Annual means have been subtracted from both the model and measurement data. Black represents CH_4 mole fractions and red represents $\delta^{13}C$-CH_4. Where there are sufficient data available in the 2005 to 2009 period, the range of observed monthly mean values relative to the annual mean is represented by a vertical bar. Dashed lines represent model results from the NO_WETLD scenario (where wetland emissions >50° N have been removed relative to BASE). Dot-dot-dash lines represent model results from the INC_WETLD~~_X2~~ scenario (where wetland emissions >50° N have been increased by 50 % relative to BASE). Variations in $\delta^{13}C$-CH_4 have been multiplied by a factor of 10.

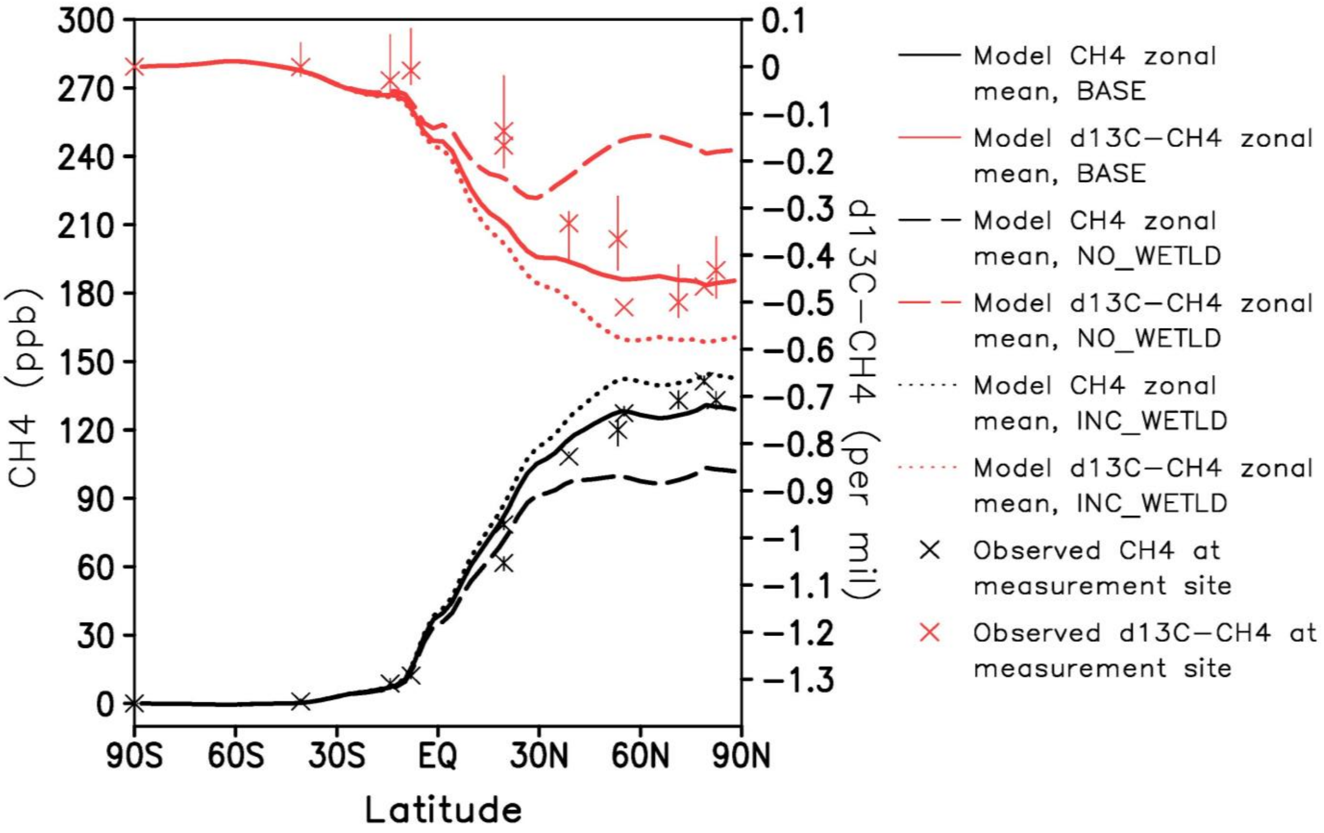

Figure 7: The difference between surface annual mean CH_4 and $\delta^{13}C-CH_4$ and South Pole annual mean values. Model results are compared to NOAA-ESRL and CU-INSTAAR observations. Black represents CH_4 mixing ratios and red, $\delta^{13}C-CH_4$ fractionations. Where there are sufficient data available in the 2005 to 2009 period, the range in annual mean station-South Pole observed differences is represented a vertical bar. Solid lines represent model results from the BASE scenario. Dashed lines represent model results from the NO_WET scenario (where wetland emissions >50° N have been removed relative to BASE). Dotted lines represent model results from the INC_WETLD~~_X2~~ scenario (where wetland emissions >50° N have been increased by 50 % relative to BASE).

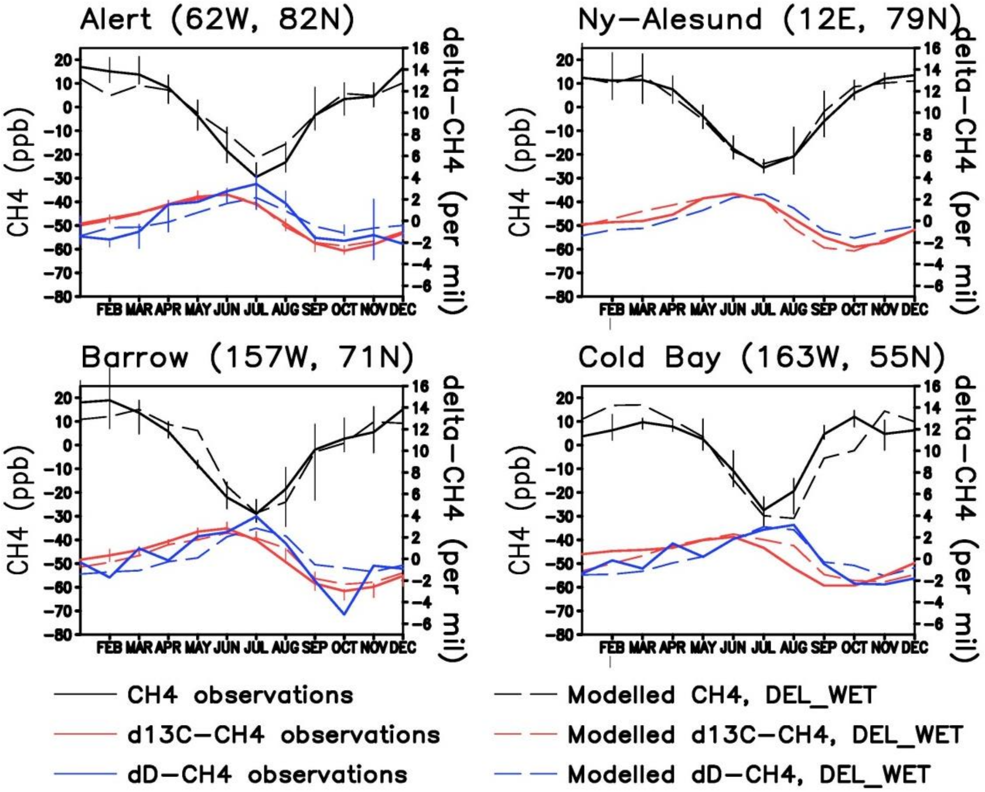

Figure 8: As Figure 5, except showing model results from the DEL_WET scenario (where the seasonal cycle of wetland methane emissions from >50° N has been delayed by one month relative to BASE). Variations in δ^{13}C-CH$_4$ have been multiplied by a factor of 10.

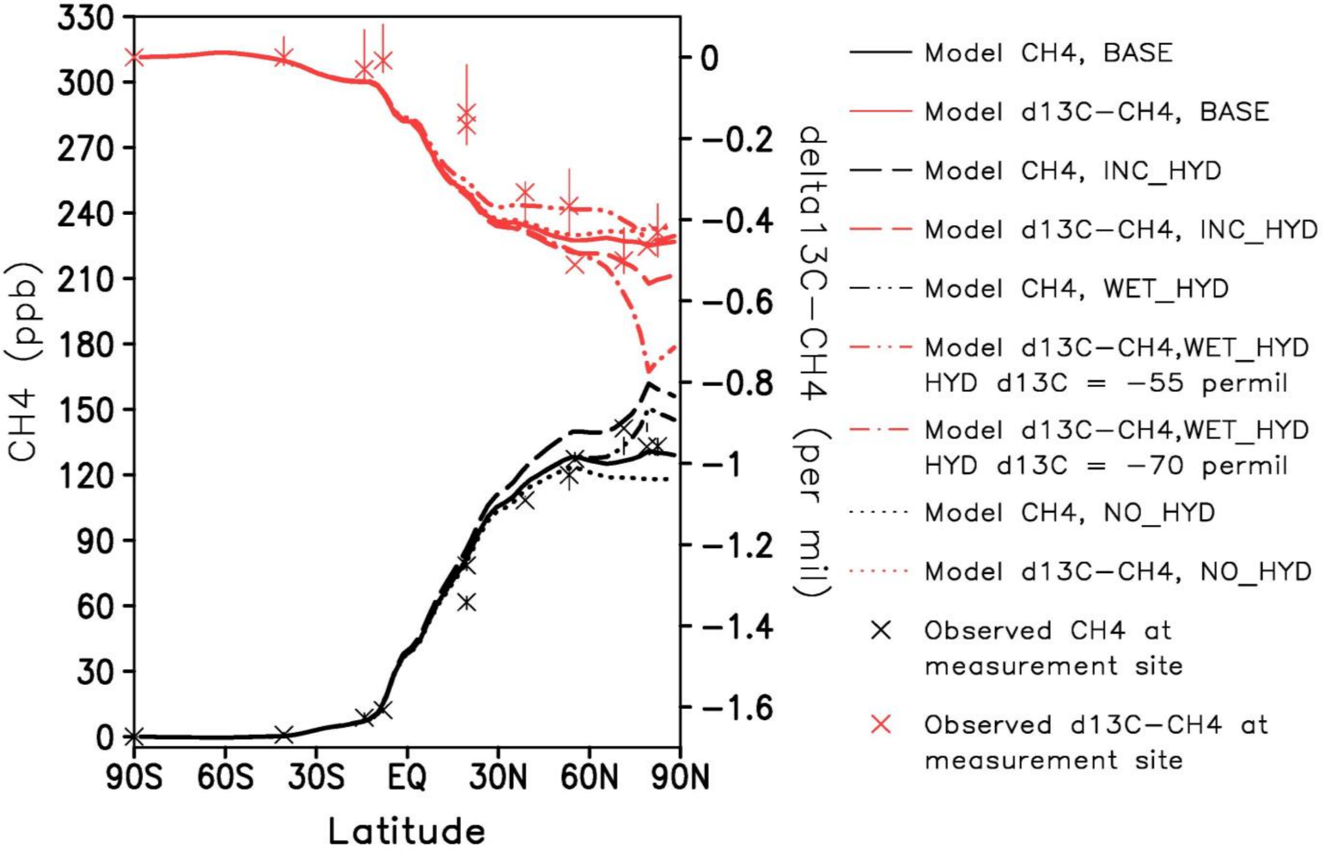

Figure 9: The difference between surface annual mean modelled latitudinal gradients in CH_4 and $\delta^{13}C$-CH_4 and South Pole annual mean values. Model results are compared to NOAA-ESRL and CU-INSTAAR observations. Black represents CH_4 mixing ratios and red, $\delta^{13}C$-CH_4 fractionations. Where there are sufficient data available in the 2005 to 2009 period, the range in annual mean station-South Pole observed differences is represented a vertical bar. Solid lines represent model results from the BASE emission scenario. Dashed lines represent model results from the INC_HYD scenario (where hydrate emissions have been increased by 12 Tg yr^{-1} to 17 Tg yr^{-1} relative to BASE). Dotted lines represent model results from the NO_HYD scenario (where emissions from methane hydrates are removed relative to BASE). Dot-dash lines show model results from the WET_HYD scenario (where hydrate emissions are increased by 12 Tg yr^{-1} to 17 Tg yr^{-1} and wetland emissions > 50° N are reduced by 12 Tg yr^{-1} relative to BASE). Dot-dot-dash lines represent emission magnitudes as for the WET_HYD scenario, but with an isotopic fractionation for hydrate emissions of -70‰.

Supplementary Material

Further details on the p-TOMCAT BASE scenario

The kinetic isotope effects for the methane reaction rates used in the model are listed in Table S1.~~and the emissions used in the pTOMCAT BASE scenario described in Table S2.~~. Prescribed surface methane fluxes from anthropogenic sources are taken from EDGAR v4.1 (http://edgar.jrc.ec.europa.eu/overview.php?v=41) for 2005. A seasonal variation has been applied to the EDGAR v4.1 fossil fuel source, following Gurney et al. (2005). Biomass burning emissions are taken from a GFEDv2 climatological average (Van der Werf et al. 2006), and are scaled to 31 Tg yr^{-1}. The geographical and temporal distribution of natural methane emissions from termites, hydrates and wetlands is taken from Fung et al. (1991). Tropical and mid-latitude wetland emissions (<50° N) are scaled to 200 Tg yr^{-1} (wetland emissions >50° N are left unscaled). Table S2 also shows the source-specific δ^{13}C and δD signatures used in the model. As for the fluxes, the isotopic signatures used are all subject to a level of uncertainty. Measurements of source δD signatures are currently much more limited than the δ^{13}C signatures and are therefore there is less information about how they vary with source type and region. Out of the δ^{13}C source signatures, there is a large uncertainty associated with the δ^{13}C isotopic signature of methane emissions to the atmosphere from subsea permafrost and hydrates. This is discussed in Section 6.3. Observations also suggest a wide geographical spread in the δ^{13}C signature of emissions from the coal industry (e.g. Zazzeri et al. 2015). In the results presented, we have used a δ^{13}C signature for emissions from the coal industry of -50 ‰. However, simulations in which emissions were assigned δ^{13}C values of both -35 ‰ and -40 ‰ only had a small impact on the modelled distribution relative to using -50 ‰ and did not influence our conclusions.

Figure S1 shows a comparison of modelled and observed seasonal cycles of methyl chloroform from the NOAA-ESRL halocarbons in situ program at Barrow, Alaska, indicating that the seasonal cycle of the model prescribed OH concentrations is well represented in the Arctic region.

References

Bergamaschi, P., Bräunlich, M., Marik, T., and Brenninkmeijer, C. A. M.: Measurements of the carbon and hydrogen isotopes of atmospheric methane at Izaña, Tenerife: Seasonal cycles and synoptic-scale variations, J. Geophys. Res., 105(D11), 14531–14546, doi:10.1029/1999JD901176, 2000.

Crowley, J. N., Saueressig, G., Bergamaschi, P., Fischer, H. and Harris, G. W.: Carbon kinetic isotope effect in the reaction CH4+Cl: a relative rate study using FTIR spectroscopy, Chemical Physics Letters, 303, 268-274, 1999.

DeMore, W. B., Rate constant ratio for the reaction of OH with CH3D and CH4, J. Phys. Chem., 97, 8564–8566, 1993.

Fung, I., John, J., Lerner, J., Matthews, E., Prather, M., Steele, L. P., and Fraser, P. J.: Three-dimensional model synthesis of the global methane cycle, J. Geophys. Res., 96, 13033-13065, doi:10.1029/91JD01247, 1991.

Gierczak, T., Talukdar, R. K., Herndon, S. C., Vaghjiani, G. L., and Ravishankara, A. R.: Rate Coefficients for the Reactions of Hydroxyl Radicals with Methane and Deuterated Methanes, The Journal of Physical Chemistry, 101 (17), 3125-3134, doi: 10.1021/jp963892r, 1997.

Gurney, K. R., Chen, Y.-H., Maki, T., Kawa, S. R., Andrews, A., and Zhu, Z.: Sensitivity of atmospheric CO_2 inversions to seasonal and interannual variations in fossil fuel emissions, J. Geophys. Res., 110, D10308, doi:10.1029/2004JD005373, 2005.

Saueressig, G., Bergamaschi, P., Crowley, J. N., Fischer, H., Harris, G. W., Carbon kinetic isotope effect in the reaction of CH4 with Cl atoms, Geophys. Res. Lett., 22, 1225–1228, doi: 10.1029/95GL00881, 1995.

Saueressig, G., Bergamaschi, P., Crowley, J. N., Fischer, H., Harris, G. W.: D/H kinetic isotope effect in the reaction CH4+Cl, Geophys. Res., 23, 3619–3622, doi: 10.1029/96GL03292, 1996.

Saueressig, G., Crowley, J. N., Bergamaschi, P., Brühl, C., Brenninkmeijer, C. A. M. and Fischer, H.: Carbon 13 and D kinetic isotope effects in the reactions of CH4 with O(1 D) and OH: New laboratory measurements and their implications for the isotopic composition of stratospheric methane, J. Geophys. Res., 106(D19), 23127–23138, doi:10.1029/2000JD000120, 2001.

Snover, A. K., *and* Quay, P. D.: Hydrogen and carbon kinetic isotope effects during soil uptake of atmospheric methane, Global Biogeochem. Cycles, 14*(*1*)*, 25–39, *doi:*10.1029/1999GB900089, *2000.*

Tyler, S. C., Rice, A. L. and Ajie, H. O.: Stable isotope ratios in atmospheric CH4: Implications for seasonal sources and sinks, J. Geophys. Res., 112, D03303, doi:10.1029/2006JD007231, 2007.

Van der Werf, G. R., Randerson, J. T., Giglio, L., Collatz, G. J., Kasibhatla, P. S., and Arellano, Jr., A. F.: Interannual variability in global biomass burning emissions from 1997 to 2004, Atmos. Chem. Phys., 6, 3423–3441, 2006.

Zazzeri, G., Lowry, D., Fisher, R. E., France, J. L., Lanoisellé, M. and Nisbet E. G., Plume mapping and isotopic characterisation of anthropogenic methane sources, Atmos. Environ. 110, 151-162, doi:10.1016/j.atmosenv.2015.03.029, 2015.

Table S1. Kinetic isotope effects for methane sinks in p-TOMCAT

Methane Sink	$KIE^{12C/13C}$	$KIE^{H/D}$
CH_4 + OH	1.0039[1]	1.29[5]
CH_4 + Cl	1.066[2,3,a]	1.508[4,a]
CH_4 + O(^{1}D)	1.013[1]	1.06[1]
Soil Oxidation	1.018[6]	1.083[6]

[1]Saueressig et al. (2001), [2]Saueressig et al. (1995), [3]Crowley et al. (1999), [4]Saueressig et al. (1996), [5]This value is within a range of quoted literature values (DeMore et al., 1993, Gierczak et al., 1997, Saueressig et al. 2001, Bergamaschi et al., 2000, Tyler et al., 2007), [6]Snover et al., (2000), [a]Kinetic isotope effects are temperature dependent, the value quoted is for 298 K.

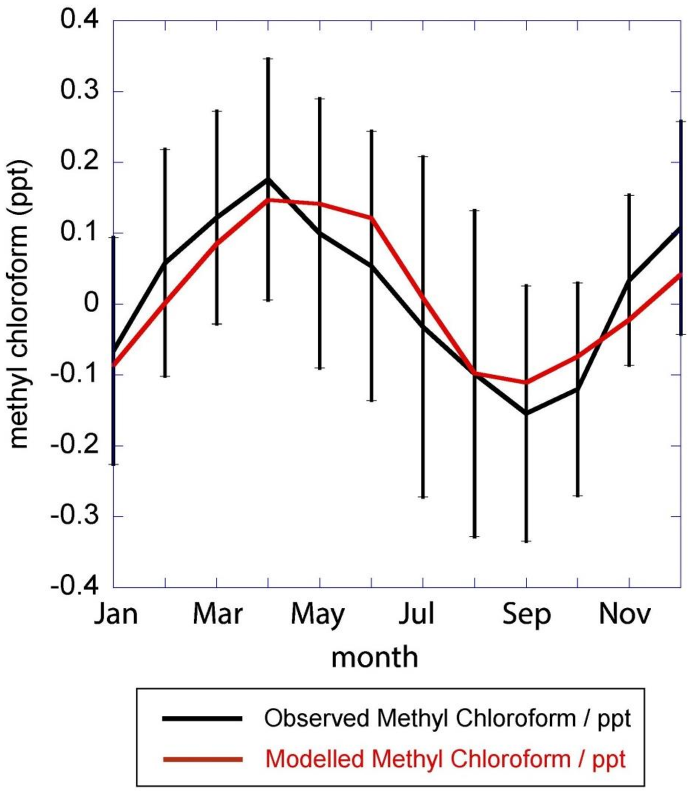

Figure S1: A comparison of observed and modelled seasonal cycles for methyl chloroform at Barrow, Alaska (157°W, 71°N). NOAA-ESRL observations are shown in black and are for the year 2009; error bars show +/- 1 s.d.. Model data uses 2009 meteorology and is shown in red. Linear trends and annual mean mixing ratios have been removed from both the observational and modelled data.

Reply to Referee #1 (bold italics).

Overview:

The manuscript “Using δ1 C-CH4 and δD-CH4 to constrain Arctic methane emissions” by Warwick et al. describes the results of a modelling study of Arctic wetland and hydrate emissions, in which the simulated concentrations of CH4, along with the associated δ13C-CH4 and δD-CH4 ratios, are compared to observations made at a number of high-latitude Northern Hemisphere measurement sites. The latitudinal gradient of these isotopologues is also assessed in comparison to observations. Finally, in an attempt to improve our current understanding of methane emissions from the Arctic, the effect of changes made to the wetland and hydrates emission inventories in the region is investigated.

Overall the manuscript is very well written, with few technical corrections necessary. The figures are generally quite clear and well chosen, although some small alterations are necessary for a couple of them. The methods used in this manuscript provide a neat way of assessing the accuracy of some of the current methane inventories used in atmospheric models, and the improvement in the comparisons with observations after the seasonal cycle of the wetland emissions is altered is striking. Using the three isotope ratios of methane as a ‘triple check’ on the seasonal cycle of the emissions works well and provides extra clues as to the timing and magnitude of emissions in the region. Finally the examination of the magnitude of hydrate emissions in the Arctic, whilst brief, does indicate that some recent estimates of emissions from this source may be too large.

My main reservation is that the conclusions drawn are dependent on a single (fairly old) wetland inventory, and there is no discussion on the impact that this fact might have on results. Is the relative geographical distribution of wetland emissions important for your conclusions to be substantiated? See general comments for more details.

I recommend this manuscript for publication after these revisions have been carried out.

We thank the referee for their very helpful comments and suggestions which have helped improve the manuscript.

Our response to the comment on our use of the Fung et al., 1991 emission inventory is included in the replies to the general comments below.

Comments:

1. Page 1, lines 20-29: These paragraphs could use some extra references. You describe the recent changes in the methane growth rate without referring to any sources for this information (‘2007... rapid methane increase’,’growth was strongest in the tropics’, etc.), and there is also no reference for the assertion that fossil fuel changes could play a role in the global growth rate or that Arctic emissions are poorly quantified.

   Several references have now been added to this paragraph (see P1, l20-28), including those for the role of fossil fuel changes. The poor quantification of Arctic emissions is discussed (and referenced) by source type in the following paragraphs of the introduction.

2. Page 5, lines 5-9: In this work, you have used observations averaged over 2005-2009 and model meteorology for 2009 only, but in order to show that the OH fields used in the study are

to some extent accurate, you show comparisons with MCF concentrations at one site for the year 2011. To be consistent with the meteorology used for the later figures, can you show 2009 concentrations here? MCF measurements should also be available at Alert, Canada. Does the model also capture the seasonal cycle that far north?

The figure has been changed to include observed MCF mixing ratios for 2009. As for the 2011 data, there is good agreement between modelled and observed seasonal cycles. As requested by Referee #2, we have now moved this figure into the supplementary information (Fig. S1).

MCF measurements are also available at Alert, however this data contains significantly more noise and lacks a smooth seasonal cycle. The model predicts a smooth MCF seasonal cycle at Alert, similar to that modelled at Barrow, but with a slightly smaller amplitude. The modelled MCF seasonal cycle at Alert compares well to the observed Alert seasonal cycle, minus the noise (i.e. capturing the approx. timing of peak/minimum mixing ratios). However, due to the additional noise in the Alert observations we have chosen to present only the Barrow data.

3. Page 5, line 16: My main reservation with this study is related to the emissions inventories used. The Fung wetland inventory is now 25 years old, and whilst it generally does a good job, I think it is worth at least discussing the idea that the distribution of emissions in this inventory may not be correct. Since all of your observation sites are located in the US and Europe, are the observed seasonal cycles sensitive to the significant emissions from Siberia, or is the cycle only of the local emissions important?

In our model simulations, high latitude northern wetland emissions from Asia, Europe and America were coloured or 'tagged' separately. Our results show us that modelled seasonal cycles at presented measurement sites are predominantly influenced by high northern latitude wetland emissions from America and/or Europe, with little sensitivity to Siberian emissions. We found that altering the Fung emission distribution in a simple way via varying the relative emission strengths associated with these regional tracers offered no improvement with the comparison to observations. Increasing the European and/or American contributions while reducing the Asian (Siberian) contribution gave a result similar to INC_WET, and vice versa to NO_WET. This information has been added to relevant sections of the manuscript (5.2.1, 6.2.1 and 7).

In the introduction we discuss the large uncertainties associated with high northern latitude wetland emissions. Given the large variability in the spatial distribution and global magnitude of emissions in both process models and inversion studies (e.g. see Table 3, Melton et al., 2013), it is hard to determine which inventory may contain the most accurate spatial distribution of emissions. Although the Fung emissions are now 25 years old, and have been proceeded by newer wetland emission estimates, it is not clear that newer estimates are necessarily better (or worse). Note that the Fung wetland emissions were used in a variety of models in the TRANSCOM studies in 2011 and 2013 (Patra et al, 2011; Saito et al., 2013).

4. Ideally, you'd carry out a supplementary model-run in which an alternative wetland scenario is used. The Bousquet (2011) inversion inventory, for example, assimilated observations of CH4 made throughout the Arctic, and would likely, therefore, be able to capture the seasonal cycle of Arctic CH4 well. However, according to Figure 1, it does not show the same delayed seasonal cycle and large magnitude of autumnal emissions required in your FUNG_DEL cycle in order to capture the seasonal cycle of CH4 . Also, as far I can tell, it has not been compared to observations of methane isotopologues before, and doing so may back up your conclusions that significant emissions deeper into the autumn are necessary.

   Unfortunately it is not possible to perform any further comparable simulations due to changes in computer platform.

   The Bousquet inversion inventory provides estimates of wetland emissions from 1993 to 2009, and it is the average of the years 1993 to 2004 that was shown in Figure 1 (these years were chosen originally to aid comparison to the WETCHIMP data). However, when considering the year by year data, there is a large inter-annual variation in total 50-90°N wetland spring-time emissions in the Bousquet dataset, with negative or very low total wetland emissions from latitudes >50°N occurring during May in many recent years. Years in which total May emissions >50°N are either negative or very low (similar to winter values) in the Bousquet dataset are: 2002, 2005, 2006, 2007, 2008 and 2009. Therefore emission data derived from the Bousquet atmospheric methane inversions supports our result for very low high latitude wetland emissions in May (and thus a later spring/summer kick-off in wetland emissions) for the 2005-2009 period. We have now changed Figure 1 to show Bousquet average emissions from the years 2005-2009 (as these are the years that we later use for observational data).

   As well as updating Figure 1, we have added a comment about the varying seasonality of the Bousquet dataset to Section 7.

5. Related to this, I note that you used the GFEDv2 biomass burning inventory. Version 4 of this inventory is now available, and any changes to the impact that the heavier δ13C-CH4 has at these locations might affect your conclusions. However, I accept that the relative contribution of biomass burning emissions compared to wetland emissions at these latitudes is probably very small and therefore unlikely to have an effect unless emissions are local to the measurements.

   We agree that ideally these simulations could be updated to use version 4 for biomass burning emissions. However, as outlined above, no further comparable model simulations are now possible. An analysis of our tagged tracers demonstrates that biomass burning emissions have a negligible impact on seasonal cycles and the latitudinal gradient at these latitudes. Therefore we do not believe updating the biomass burning emission inventory would alter our conclusions.

6. If further simulations are not possible, I think a discussion of the effect of your choices on your results should be included in the results section.

We assume this comment is aimed principally at our choice of wetland emission dataset (an issue also brought up by Reviewer 2). We have replied to these comments above and added further information to the manuscript about spatial/temporal emission distributions in both the Bousquet dataset (as requested by Reviewer 1) and the LPJ-Bern dataset (as requested by reviewer 2), see Section 6.2.2, Section 7.

In addition, in Figure 2, we have added a new panel providing more information on the latitudinal variation in emission seasonal cycles in the Fung et al. dataset. We found that varying the spatial distribution of high latitude northern wetland emissions in the Fung dataset in a simple way did not improve the comparison with atmospheric observations (please see also our reply to referee #1's comment no. 3 and referee #2's comment no. 1).

7. Page 5, line 16: This is the first mention of the BASE scenario. You should make explicit that here, 'BASE' refers to the control experiment that uses the emissions described in the previous section, rather than some model set-up.Page 6, line 6-10: This paragraph needs a little more detail. You have not previously described the locations of those measurements made further south than Cold Bay (perhaps they could also be included in Figure 4?). You say that the gradient in δD-CH 4 is captured, and also that it is underestimated in the NH mid latitudes. Can you explain more clearly? It looks to me that perhaps the δD-CH 4 is mostly captured quite well as far to 50S, but that using the South Pole value as a baseline is shifting the model away from the observations. Perhaps it's the SH gradient that isn't captured, rather than the NH gradient?

   The text has been changed to read 'BASE control scenario' to make this clearer.

   We agree with the referee's comments regarding the δD-CH 4 latitudinal gradient. The paragraph discussing this at the end of Section 5.1 has been expanded.

   A description of the other measurement sites used in this study has been added to Section 2 and their locations plotted on the previous Figure 4 (now Figure 3).

8. Page 8, line 12: It's a shame that there are no δD-CH 4 ratios included here for completeness, but since the changes to the wetland emissions in this section of the study don't improve simulated CH 4 or δC 13 -CH 4 concentrations, I understand the reluctance to carry out the runs.

   As previously mentioned, unfortunately no further comparable runs are possible at this point.

9. Page 8, line 18: The name "WETLD_X2" is a little misleading, as emissions have been increased only by 50%. Can you change this name?

   We have changed the name of this scenario to INC_WETLD.

10. Page 11, line 15: Are the model lines here full zonal means across all longitudes? If so, is there any impact on the comparisons at the sites in the Arctic if you compare only at the

measurement locations? I think the plot would be too busy if you included these comparisons within it, but you could mention it in the text if there is any effect.

Yes, these are full zonal means. We did initially include the measurement location data, but as suggested by the reviewer, the plot became too busy and so it was removed before submission. As requested, we have now added some text to Section 6.3 describing the impact of using model data from measurement station locations rather than zonal means (and to make it clear zonal means are plotted).

11. Figure 3: I think that this plot could be a little clearer. Can you include the locations of the measurement sites here (or in Figure 4)? Is this an annual mean or is it the peak summertime emissions? Can you differentiate between regions where wetland emissions are zero and where they're just smaller than the lowest value in your colourbar?

    We have added the location of the measurement sites to the previous Figure 4 (now Figure 3) as it enables all sites to be included. The Figure caption has been updated to clarify annual mean emissions are shown. The colourbar has been changed to differentiate regions where wetland emissions are zero.

12. Perhaps you could include a similar second panel showing the standard deviation of the emissions, or the month during which emissions peak (or at least mention it in the text)? i.e. do emissions peak in July everywhere in the Artic, or does it vary by region?

    We have now included a second panel in Figure 3 that shows zonally summed emissions for each of the summer emission months (seasonality does not vary greatly with longitude). For latitudes < ~70°N, emissions peak in July. For latitudes > ~70°N, emissions are fairly constant for the June-August period, and decline slightly for September.

13. Figure 10: Can you differentiate the lines more clearly in this plot? The difference between the dash, dot, dot-dash and dot-dot-dash lines is not obvious enough in a plot of this size (especially as they only deviate in a small subsection of latitudes).

    We have now tried using various different line types and colours for this figure. In our opinion the best improvement was obtained by swapping some of the line types in the legend and increasing the length of the y-axis.

Technical corrections:

Page 1, line 11 and throughout: I find the use of the term ‘coloured’ throughout the manuscript to describe the different tracers a bit odd, although I accept that it can be a difficult idea to describe well. I'd suggest changing to the term ‘tagged’ or similar for clarity.
Text changed to read ‘tagged’.

Page 2, line 3: “to-date” -> “to date” (no hyphen)
Changed.

Page 12, line 29: “May-time emissions” -> “May emissions”/“emissions than predicted in May”
Changed.

Page 13, line 13: “currently lacking” -> “currently-lacking”
Changed.

Replies to Referee #2 (bold italics).

General

The manuscript 'Using d13C-CH4 and dD-CH4 to constrain Arctic methane emissions' by Warwick and co-workers presents a study of atmospheric CH4 and its isotopes (d13C and dD) in the Arctic. Model simulations of all three components together with observations are used in a qualitative way to draw conclusions on the main arctic emission sources and their seasonal behavior. The analysis applies state-of-the-art modeling techniques and the methods and results are generally presented with a clear language and structure. The work clearly adds an important piece of information entangling the contributions of different methane sources and will probably help to further improve process models that are of paramount importance to understand future climate-emission feedbacks in the Arctic. I only have a few minor comments that can be addressed in the revised text but will, most likely, not require any major changes in the analysis.

We thank the referee for their very helpful comments and suggestions which have helped improve the manuscript.

Major comments

1. One possibly more important remark has to do with the chosen wetland emissions in the presented simulations. Why was the rather old Feng et al. dataset chosen as a reference? As can be seen in Figure 1 the LPJ-Bern emissions already follow the suggested delay in summer-time emissions. Related to this: What is the influence of the spatial distribution of the chosen wetland emissions. Could the suggested shift in emissions also stem from an erroneous distribution in space rather than in time? How different is the spatial distribution of LPJ-Bern as compared to Feng et al?

   We followed the TRANSCOM model comparisons (Patra et al., 2011, Saito et al. 2013) in using the Fung et al. (1991) wetland dataset. Although there are now quite a few published wetland methane emission datasets available (see Fig. 1), uncertainties are large and it is not clear which dataset may be the most accurate or best performing.

   We performed a simple analysis to investigate whether an erroneous emission distribution, rather than emission seasonality, could influence the modelled seasonality of methane mixing ratios etc. at the chosen measurement sites. Our model includes 4 wetland methane tagged tracers: north European, north American, north Asian and tropical. We tried varying the relative quantities of northern emissions (e.g. decreasing north American and/or north European while increasing Asian/Siberian emissions) and varying the relative quantities of northern vs. tropical emissions. However, the model results were very similar to either the INC_WET or NO_WET scenarios and we were unable to capture observed seasonalities in mixing ratios and/or isotopic ratios (see also our reply to referee #1's comment no. 3).

   It is possible that inaccuracies in the emission distributions within our tagged regions could also impact modelled mixing ratio seasonalities. For example, if the model had a

greater proportion of emissions >50°N located at very high latitudes, total emissions >50°N during May could be reduced (see new Fig. 2b). However, this would also have the unwanted impact of reducing emissions during October (Fig. 2b) and would alter the modelled latitudinal gradient (which is currently well captured, Fig 4). Therefore we believe it would be very difficult to correct the modelled atmospheric seasonal cycles by altering only wetland emission distributions and not seasonalities.

There are differences between the spatial distribution of emissions in the LPJ-Bern model and Fung et al., (1991), however the main emission hotspots are in broadly the same locations (West Siberia, Northern Europe, Hudson Bay lowlands). The differences in spatial distribution do not appear to be the cause of the different summed 50-90°N seasonalities between the 2 datasets, as the delayed seasonal cycle in the LPJ_Bern dataset relative to the Fung dataset is a consistent feature across all high latitude northern locations. In the Fung dataset, summed zonal mean September emissions are lower than corresponding emissions in the peak emission months of June, July and August, across all latitudes >50N (see Fig. 2). However, In the LPJ-Bern dataset, zonally summed June emissions are lower than corresponding emissions in the peak emission months of July, August and September, across all latitudes >50°N (not shown). We have added this information to the manuscript at the end of Section 6.2.2 (P10, l21-29).

Minor comments

2. P1, l18/19: Clarify if by inventories you are referring to purely anthropogenic emissions here.

   This is now clarified in the text to read 'anthropogenic or wetland emission inventories'. Whether anthropogenic or wetland emissions are implicated depends upon the seasonality and isotopic fractionation of the ESAS source.

3. P1, l26: What is the status of the Nisbet et al. publication? If not yet published another reference is needed here.

   The Nisbet paper has now been published in GBC. The manuscript and reference list has been updated.

4. P2, l33: 'In this study': Does this still refer to Berchet et al. or the current study?

   This refers to Berchet study. The text has been changed to clarify this.

5. P3, l6/7: The given reference is rather old. Please give some newer references and a total amount of emissions here. See for example Kirschke et al. 2013 for some numbers and additional references.

   A newer reference (EDGAR v4.2) has been added.

6. P3, l8: The additional stratospheric sink by Cl and O1D should be mentioned here as well, although it probably adds little to the seasonality.

   The stratospheric Cl and O1D sink is now listed here.

7. P3, l22-24: You should mention the work by Rigby et al. here as well, who already ran a CH4 isotope model (both d13C and dD) to evaluate the benefits of atmospheric isotopic observations: Rigby et al. 2012, JGR, VOL. 117, D12312, doi:10.1029/2011JD017384.

   This study has been mentioned elsewhere in the manuscript, however we agree it would be appropriate to mention it her again and have added another reference to the Rigby study at this point.

8. P3, l30f: In figures 5, 8 and 10 more than these 4 sites are used for comparison. Please mention which other sites are used in the figures.

   Further information regarding the additional measurement locations in figs 5, 8, and 10 has now been added to Section 2. Their locations are now shown in Figure 3.

9. P4, l16-18: For which period are these values given?

   The period 2005 to 2009. This information has been added to the text.

10. P5, l2: Which functional relationship was actually used to calculate the OH reaction rate coefficient? Reference or equation.

    Relevant references for the OH, Cl and O1D reaction rate coefficients have now been added to the manuscript in Section 4.

11. P5, l9f: To put the importance of these other reactions into perspective, could you give an average lifetime of CH4 wrt to stratospheric and MBL reactions as well?

    Lifetimes for the MBL and stratospheric reactions have now been included in Section 4.

12. P5, Table S2: Table S2 should be integrated in the main paper, since it is an essential information for the study. However, in the table it should be clarified which source is taken from which reference and how seasonality is considered.

    Table S2 has been moved into the main paper (Table 1), and each source referenced.

13. P5, l24f: Which influence may the spin-up still have on the results. The spin-up basically leads to an initial state in which sources and sinks are in equilibrium. Is this adequate for the study period or could it be important to start from a background that is not in perfect equilibrium (due to steadily increasing emissions in reality).

In this study we have spun up the model using anthropogenic emission data from 2005, and compared to atmospheric observations from 2005 to 2009. During the period 2000-2007, methane mixing ratios remained approximately constant in the atmosphere (excluding seasonal variations) and the global growth rate was close to zero suggesting the methane budget was approximately in equilibrium.

Prior to the year 2000, and post 2007, atmospheric methane levels increased, indicating a disequilibrium in the methane budget. This disequilibrium is not represented in our scenarios. Due to the long lifetime of methane, it is possible that changes is emissions pre-2000 could influence atmospheric mixing ratios post-2005, however this would be more likely to impact inter-annual methane trends than the seasonal variations considered in this paper.

Due to uncertainties in interannual methane emission trends, that the period considered in the paper occurs towards the end of an apparent period of equilibrium in the methane budget, and that we are considering seasonal variations rather than year to year trends, we believe that a spin up using yearly constant methane emissions is justified in this case.

14. P6, l22: 'with the seasonal cycle'. Does this refer to the observed seasonal cycle?

    Text has been changed to read 'observed seasonal cycle'.

15. P9, l2f: Fig. 1 should be mentioned here again, which shows the emission profiles of Fung and Fung delayed.

    A reference to figure 1 has now been included.

16. P9, l6: 'forward': To me this is confusing. I would call it shifting the seasonal cycle backward.

    We wrote 'one month forward' as April emissions have been moved to May, May to June etc.. In order to be less confusing we have removed the phrase 'forward in the year' and instead said 'delayed by one month'.

17. p10, l1-3: Berchet et al. 2016 clearly showed a strong seasonal cycle for emissions from ESAS, with a summertime peak in the order of what was suggested by Shakhova et al. 2012 for the whole year (see Fig. 5 in Berchet et al. 2016), i.e. 10-15 Tg/yr. In contrast, Berchet et al. suggest close to zero emissions in winter. How could this seasonality, that was not considered in the current model analysis, change the drawn conclusions concerning the impossibility to accommodate the ESAS flux as suggested by Shakhova et al.?

    We believe this point is already partially covered by summary points (a) and (b) in Section 6.3. They outline that, to accommodate a large ESAS source, our model requires a reduction in either high latitude wetland emissions or high latitude anthropogenic emissions, depending on whether ESAS emissions are considered to be seasonal or aseasonal, and the value chosen for their δ^{13}C isotopic composition.

A strong summertime peak for the ESAS emissions would resemble the seasonality for high latitude northern wetlands, which are also predicted to peak in the summer. Therefore, including such a seasonal cycle for ESAS emissions would make it harder to distinguish between ESAS and high latitude wetland emissions in our model simulations, particularly if ESAS were assigned a very negative δ^{13}C isotopic signature (~-70‰), similar to high latitude wetlands.

We have added further information to the manuscript regarding the possible impacts of a seasonal ESAS source in Section 6.3 (P12, l7-9 and P12, l30 – P13).

18. Section 6.2: Please comment on the good agreement of the delayed temporal development used in your sensitivity run and that simulated by LPJ-Bern (as seen in Fig. 1). Does their model version already include possible CH4 emissions after freezing of the top soil?

The WETCHIMP-WSL model intercomparison (Bohn et al. 2015) compared emissions from all the WETCHIMP models in the West Siberian region. The late peak in LPJ-Bern emissions was also identified in this study, and was found to be predominantly due to a late peak in wet mineral soil emission intensity, despite a very late peak in CH4-producing area. We have added this information to the discussion in Section 6.2.2 (final paragraph).

19. P11, l21-23: This thought should be given some more discussion. Would it still be possible to accommodate a 50 % reduction in high-latitude anthropogenic emissions (as compared with the BASE run) within the range given by previous studies (e.g. Kirschke et al.).

The -50% value given was an error. Anthropogenic emissions >50N total 36 Tg/yr in our scenario. If hydrate emissions are increased by 12 Tg/yr (from 5 to 17 Tg/yr), a 12Tg/yr reduction in anthropogenic emissions would be equate to a 33% reduction. This has been corrected in the text. A reduction of this magnitude would remain within the range of top-down and bottom studies studies presented in Kirschke et al. review paper, although be very close to the lower estimates given for the agri-waste and fossil sources. (Biomass burning only represents a small proportion of emissions at these latitudes.) This information has been added to the manuscript in Section 6.3 (P13,l14-19).

20. Figure 2: Should be part of the supplement. It is not essential to the study, but 'only' demonstrates that the applied model seems to perform reasonably well in terms of OH degradation.

Figure 2 has been moved to supplementary information.

21. Figures 6 and 9: Why is there no observed dD for Ny-Alesund? If it was not observed there, it should be mentioned somewhere in the text.

dD was observed at Ny-Alesund. However after quality control, there was not sufficient data to be able to plot a seasonal cycle. This has now been explained in the caption for Fig. 6.

22. Adding a table summarizing all model runs (BASE and sensitivities) and their specific settings would be nice. All the sensitivities should be given an abbreviation/name (not done in all cases) in this table and in the text so that it is easier to quickly identify what the specifics of a certain run

A Table summarising all model runs has now been added to the manuscript (Table 2).

References

Patra, P. K., Houweling, S., Krol, M., Bousquet, P., Belikov, D., Bergmann, D., Bian, H., Cameron-Smith, P., Chipperfield, M. P., Corbin, K., Fortems-Cheiney, A., Fraser, A., Gloor, E., Hess, P., Ito, A., Kawa, S. R., Law, R. M., Loh, Z., Maksyutov, S., Meng, L., Palmer, P. I., Prinn, R. G., Rigby, M., Saito, R., and Wilson, C.: TransCom model simulations of CH4 and related species: linking transport, surface flux and chemical loss with CH4 variability in the troposphere and lower stratosphere, Atmos. Chem. Phys., 11, 12813-12837, doi:10.5194/acp-11-12813-2011, 2011.

Saito, R., et al., TransCom model simulations of methane: Comparison of vertical profiles with aircraft measurements, J. Geophys. Res., 118, 3891-3904, doi:10.1002/jgrd.50380, 2013.